

**ROLE OF DUAL-ENERGY CT IN THE DETECTION OF
PULMONARY EMBOLISM**



THESIS

Submitted to

All India Institute of Medical Sciences, Jodhpur

In partial fulfilment of the requirement for the degree of

Doctor of Medicine (MD)

(Radiology)

**July 2020
AIIMS, Jodhpur**

Dr. Satish Kumar

**ROLE OF DUAL-ENERGY CT IN THE DETECTION OF
PULMONARY EMBOLISM**



THESIS

Submitted to

All India Institute of Medical Sciences, Jodhpur

In partial fulfilment of the requirement for the degree of

Doctor of Medicine (MD)

(Radiology)

**July 2020
AIIMS, Jodhpur**

Dr. Satish Kumar

AIIMS JODHPUR

Dr. Satish Kumar

July, 2020

Name of Candidate	Dr. Satish Kumar
Address of Candidate	AIIMS Residential Complex, Jodhpur, Rajasthan, 342005
Training Institute	All India Institute Of Medical Sciences, Jodhpur
Course and Study of Subject	MD Radiology
Date of Admission To Course	July 2020
Title of Thesis	Role of Dual Energy Computed Tomography (DECT) in Pulmonary Embolism
SIGNATURE OF CANDIDATE	
Name And Designation of Guide	Dr. Pawan Kumar Garg Additional Professor Department of Diagnostic and Interventional Radiology AIIMS Jodhpur
SIGNATURE OF GUIDE	
Name and Designation of Co-Guide	Dr. Rengarajan Rajagopal Assistant Professor Department of Diagnostic and Interventional Radiology AIIMS Jodhpur
SIGNATURE OF CO-GUIDE	

Name and Designation of Co-Guide	Dr. Pushpinder Singh Khera Professor and Head Department of Diagnostic and Interventional Radiology, AIIMS Jodhpur
SIGNATURE OF CO-GUIDE	
Name and Designation of Co-Guide	Dr. Nishant Kumar Chauhan Additional Professor Department of Pulmonary Medicine AIIMS Jodhpur
SIGNATURE OF CO-GUIDE	
Name and Designation of Co-Guide	Dr. Surender Deora Additional Professor and Head Department of Cardiology AIIMS Jodhpur
SIGNATURE OF CO-GUIDE	
Name and Designation of Co-Guide	Dr. Gopal Krishna Bohra Additional Professor Department of AIIMS Jodhpur
SIGNATURE OF CO-GUIDE	
Name and Designation of Co-Guide	Dr. Sadik Mohammed Additional Professor Department of Anaesthesiology and Critical care AIIMS Jodhpur
SIGNATURE OF CO-GUIDE	

Registration of Dissertation

Certificate

This is to certify that work entitled “**Role of Dual-Energy CT in the detection of Pulmonary Embolism**” between January 2021 to June 2022, which is being submitted as a protocol for the plan of thesis towards MD in Radiology, will be carried out by Dr. Satish Kumar in the Department of Diagnostic and Interventional Radiology at AIIMS, Jodhpur under our supervision and guidance. The technique embodied in this protocol will be undertaken by the candidate himself, and the observation will be checked and verified by us from time to time.

Guide

Dr. Pawan Kumar Garg
Additional Professor
Department of Diagnostic and Interventional Radiology,
AIIMS Jodhpur

Co-Guides

Dr. Rengarajan Rajagopal
Assistant Professor
Department of Diagnostic and Interventional Radiology
AIIMS Jodhpur

Dr. Pushpinder Singh Khera
Professor and Head
Department of Diagnostic and Interventional Radiology
AIIMS Jodhpur

Dr. Nishant Kumar Chauhan
Additional Professor
Department of Pulmonary Medicine
AIIMS Jodhpur

Dr. Surender Deora
Additional Professor
Department of Cardiology
AIIMS Jodhpur

Dr. Gopal Krishna Bohra
Additional Professor
Department of General Medicine
AIIMS Jodhpur

Dr. Sadik Mohammed
Additional Professor
Department of Anaesthesiology and Critical care
AIIMS Jodhpur

DECLARATION

I hereby declare that the thesis titled “**ROLE OF DUAL-ENERGY CT IN THE DETECTION OF PULMONARY EMBOLISM**” embodies the original work carried out by the undersigned at All India Institute of Medical Sciences, Jodhpur.

Dr. Satish Kumar

Department of Diagnostic and Interventional Radiology

All India Institute of Medical Sciences

Jodhpur

ACKNOWLEDGEMENT

As this rollercoaster journey of thesis submission comes to a close, I want to take a moment to thank all those souls who have lent a helping hand directly or indirectly.

First and foremost, thanks to my parents and brother, who have always been my backbone and believed in me, no matter what.

I extend my hearty gratitude to Dr. Pawan Kumar Garg for being my guide, helping me choose this common yet uncommonly studied entity, igniting my interest in Interventional Radiology, providing all necessary support, and guiding me throughout the PG career.

I am also indebted to my co-guides, Dr. Pushpinder Singh Khera, Dr. Rengarajan Rajagopal, Dr. Nishant Kumar Chauhan, Dr. Surender Deora, Dr. Gopal Krishna Bohra, Dr. Sadik Mohammed for their support and guidance.

I also thank Dr. Taruna Yadav, Dr. Binit Sureka, and Dr. Sarbesh Tiwari for their support which created a nurturing environment, thereby helping create this work.

Hats off to my AIIMS Radiology family, aptly called the “Children of Roentgen,” my seniors, co-PGS, and juniors for all you have done.

My sincerest thanks to all the senior residents, who work alongside me all the time, guiding and helping me in all aspects. Special thanks to Dr. Ankit Grewal, Dr. Aanchal Gupta, and Dr. Himanshu for their invaluable help.

Cheers to the Radiology nursing staff and technologists for their honest work and friendly nature.

Last but not least, thanks to all my patients, without whom this study would be nothing but blank paper.

Dr. Satish Kumar

TABLE OF CONTENTS

Sr. No.	Topic	Page number
1.	Abbreviations	1
2.	Introduction	2-4
3.	Pulmonary arterial anatomy	5-7
4.	Risk factors for pulmonary embolism	8-9
5.	Medical history	10
6.	Review Of Literature	11-18
7.	Aims and objectives	19
8.	Materials and methods	19-21
9.	Dual-energy computed tomography (DECT)	22-27
10.	CT angiographic findings of acute and chronic pulmonary embolism	28-33
11.	Data collection and Statistical analysis	34
12.	Results	35-51
13.	Discussion	52-55
14.	Image Gallery /Cases	56-65
15.	Conclusion	66
16.	Limitations of study	67
17.	Bibliography	68-73
18.	<ul style="list-style-type: none">• Patient Information Sheet (English)• Patient Information Sheet (Hindi)• Informed consent form (English)• Informed consent form (Hindi)• IEC Certificate	74 75 76 77 78

LIST OF FIGURES

Sr. No	Title
1.	MIP image of CTPA showing main left and right pulmonary arteries
2.	MIP image of CTPA showing branches of right pulmonary artery
3.	MIP image of CTPA showing branches of left pulmonary artery
4.	Dual x-ray source geometry
5.	Images showing contrast to noise ratio at 100 keV and 140 keV
6.	Artifacts in dual-energy pulmonary perfusion imaging
7.	Features of acute pulmonary thromboembolism
8.	Features of chronic pulmonary thromboembolism
9.	Bar graph showing age wise cases distribution in 2 groups of study
10.	Bar graph showing gender distribution of cases in 2 groups of study
11.	Bar graph showing the status of pulmonary embolism in 2 groups of the study
12.	Bar graph showing radiation dose in 2 groups of study
13.	Bar graph showing the correlation of D-dimer and status of pulmonary embolism
14.	Bar graph showing the age-wise distribution of patients with acute and chronic thromboembolism scanned in dual-energy protocol
15.	Pie chart showing the proportion of various sites of thrombotic occlusion in patients with acute pulmonary embolism scanned in dual-energy protocol

16.	Bar graph showing the proportion of patients of acute pulmonary embolism with various sites of thrombotic occlusion showing perfusion defect on iodine maps and scanned in dual-energy protocol
17.	Pie chart showing the proportion of various sites of thrombotic occlusion in patients with chronic pulmonary embolism and scanned dual-energy protocol
18.	Bar graph showing the proportion of patients of chronic pulmonary embolism with various sites of thrombotic occlusion showing perfusion defect on iodine maps and scanned dual-energy protocol
19.	Pie chart showing the fraction of patients with acute pulmonary embolism having a history of acute DVT and scanned in dual-energy protocol
20.	Images showing acute pulmonary embolism at various levels and correlation with iodine maps
21.	Images showing chronic pulmonary embolism at various levels and correlation with iodine maps

LIST OF TABLES

Sr. No	Title
1	The mortality rate of acute pulmonary embolism according to Czech and European Guidelines
2	Risk factors of venous thromboembolism, according to the British Thoracic Society, 2003
3	Age-wise case distribution group in 2 groups of the study
4	Gender distribution of the cases in 2 groups of the study

5	Status of pulmonary embolism in 2 groups of the study
6	Comparison of radiation dose between 2 groups of study
7	Comparison of D-dimer and status of pulmonary embolism
8	Age-wise distribution of patients with acute and chronic thromboembolism and scanned in dual-energy protocol
9	The proportion of various sites of thrombotic occlusion in patients with acute pulmonary embolism scanned in dual-energy protocol
10	The proportion of patients of acute pulmonary embolism with various sites of thrombotic occlusion showing perfusion defect on iodine maps and scanned in dual-energy protocol
11	The proportion of various sites of thrombotic occlusion in patients with chronic pulmonary embolism scanned in dual-energy protocol
12	The proportion of patients with chronic pulmonary embolism with various sites of thrombotic occlusion showing perfusion defect on iodine maps and scanned in dual-energy protocol

ABBREVIATIONS

MDCT- Multidetector Computed Tomography

DECT- Dual-Energy Computed Tomography

CTPA- Computed Tomography Pulmonary Angiography

PE- Pulmonary Embolism

CTA- Computed Tomography Angiography

DEPI- Dual-Energy Perfusion Imaging

mAs- Milli ampere second

kVp- Kilovoltage peak

MIP- Maximum Intensity Projection

VTE- Venous Thromboembolism

FOV- Field of View

DVT – Deep Venous Thrombosis

V/Q- Ventilation Perfusion Scan

PBV- Perfused Pulmonary Blood Volume

ECG – Electrocardiography

mSv- millisievert

CTOI- Computed tomography obstructive index

Introduction

Pulmonary embolism (PE) is a potentially fatal disease with varying clinical presentations. As the third most prevalent cardiovascular illness (1), pulmonary embolism is associated with high morbidity and mortality. Annually, more than 650 000 cases of pulmonary embolism (PE) are documented, with an estimated 300 000 deaths. PE is the third most common cause of mortality in the USA (2) based on this occurrence level. If the diagnosis or treatment is postponed, the prognosis could be deadly. Therefore, a quick diagnosis can significantly lower mortality by enabling prompt treatment. The current gold standard for diagnosing acute PE is computed tomography pulmonary angiography (CTPA) (3). A missed PE carries a high potential risk for future venous thromboembolism. On the other hand, false-positive results and subsequent anticoagulation treatment can result in complications. The potential for overdiagnosis of PE is as harmful as underdiagnosis (4).

Ventilation/perfusion scintigraphy and traditional pulmonary angiography are currently being replaced with multidetector CT (MDCT) pulmonary angiography for assessing potential PE. In 2007, MDCT angiography was accepted as the reference standard for the diagnosis of acute PE (2). Regrettably, traditional MDCT angiography only offers morphological details, and its ability to evaluate subsegmental pulmonary arteries is inconsistent: sensitivities range from 37-96% (2). With improvements in MDCT technology, it is now possible to evaluate subsegmental pulmonary arteries.

Many technological issues that previously restricted the use of DECT pulmonary angiography were resolved in 2006 with the development of a dual-source CT system (Somatom Definition, Siemens Medical Solutions) with two x-ray tubes and two detector rows installed in the same gantry. This approach allows for the simultaneous capture of spiral images at various kV exposures during the same periods of contrast enhancement. In order to make use of the K-absorption edge of iodinated contrast material, where iodine exhibits highly different degrees

of attenuation at these two photon energies, the tubes are often adjusted to 140 kV and 80 kV. Different X-ray spectra are used in DECT to display the absorption properties of various types of materials. It is possible to selectively view materials like calcium and iodine, particularly those with large atomic numbers. Due to this, DECT can be used to see how iodinated contrast agents are distributed locally in various organs and tissues, including the brain, lungs, liver, and kidneys. It can be expected that the local blood flow coincides with the tissue iodine distribution during the first pass of a contrast agent bolus administered for CTA (5).

Similar to other diagnostic methods, including pulmonary angiography and V/Q lung scan, the primary limitation of CTPA is the detection of PE at the segmental and subsegmental levels (6).

Recent research has demonstrated that using DECT to diagnose segmental and subsegmental pulmonary thromboembolisms offers incremental benefits (1), which can drastically alter patient care and outcome.

Compared to traditional CT angiography, DECT angiography enables simultaneous evaluation of the pulmonary vasculature and parenchymal iodine distribution without excessive radiation dosage. The advantage of DECT imaging is that distant parenchyma contrast enhancement defects can be as large as 3-5 cm in diameter when caused by subsegmental emboli of 3-5 mm in diameter. Because small occlusive clots may cause more hemodynamic compromise than bigger nonocclusive ones, it would be beneficial for determining the functional relevance of emboli (7). When the initial scan enhancement is insufficient, the capacity of DECT to create virtual, low X-ray energy, monoenergetic pictures might boost vascular contrast and enable the evaluation of the pulmonary arteries (7). On specific iodine concentration maps, regional lung perfusion abnormalities can be seen in relation to this.

Our study's objective is to analyze the role of DECT in pulmonary embolism and evaluate its potential advantages over CTPA as it is currently practiced.

Pulmonary arterial anatomy

- The right pulmonary artery arises from the right ventricle and divides the left and right pulmonary arteries.
- The main pulmonary artery lies posterior, superior, and left to the aorta.
- Right and left pulmonary arteries divide into two lobar arteries, then segmental and subsegmental arteries.
- Segmental and subsegmental arteries run parallel to the bronchus and are named according to bronchopulmonary segments.

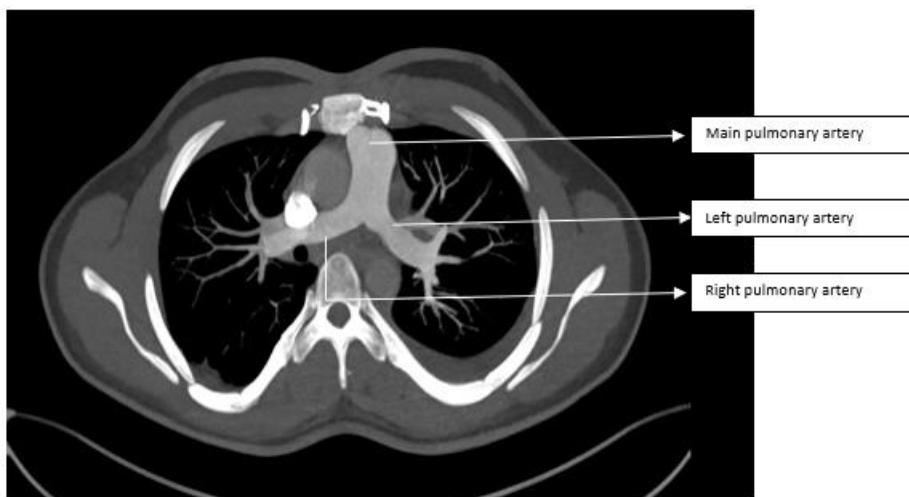


Figure 1: MIP image of CTPA showing main, left, and right pulmonary arteries

Right Pulmonary Artery

- Within the pericardium for three fourth of its length.
- Lies anterior and inferior to right main stem bronchus.

Gives two branches:

1. Truncus anterior -> supplies right upper lobe
2. Interlobar pulmonary artery -> supplies right middle and lower lobe

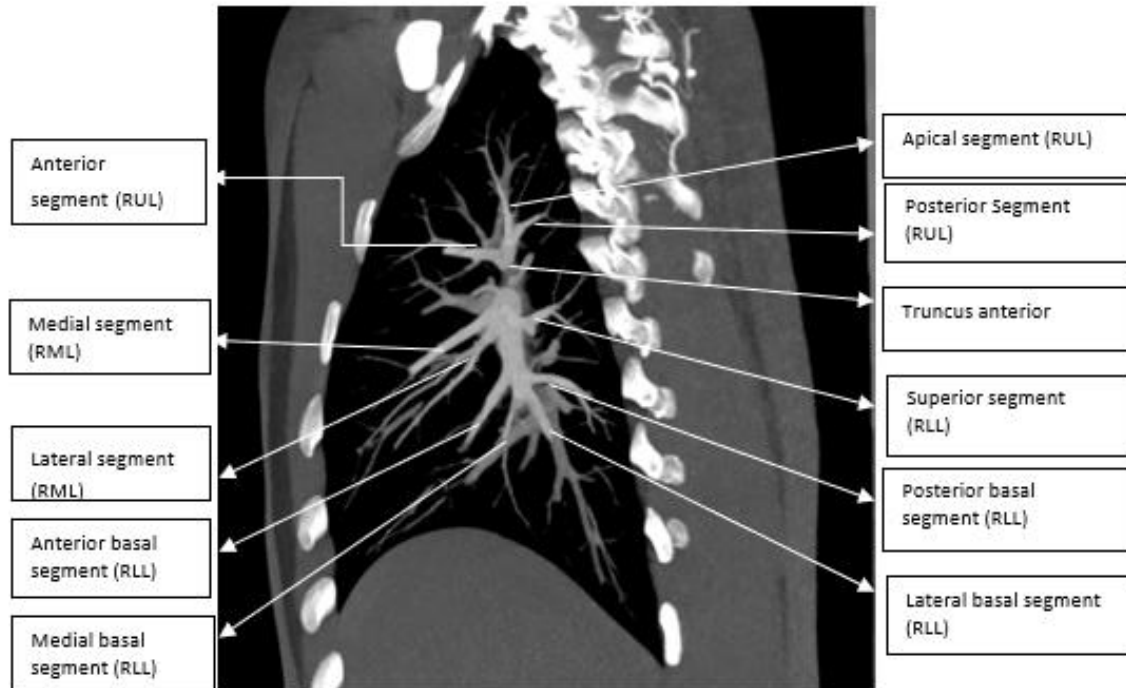


Figure 2: MIP image of CTPA showing branches of the right pulmonary artery

Left Pulmonary Artery

- Exits pericardium below aortic arch, at the ligamentum arteriosum
- Arches over and behind left main stem bronchus
- It continues as a common basal trunk and terminates into branches to basal segments.

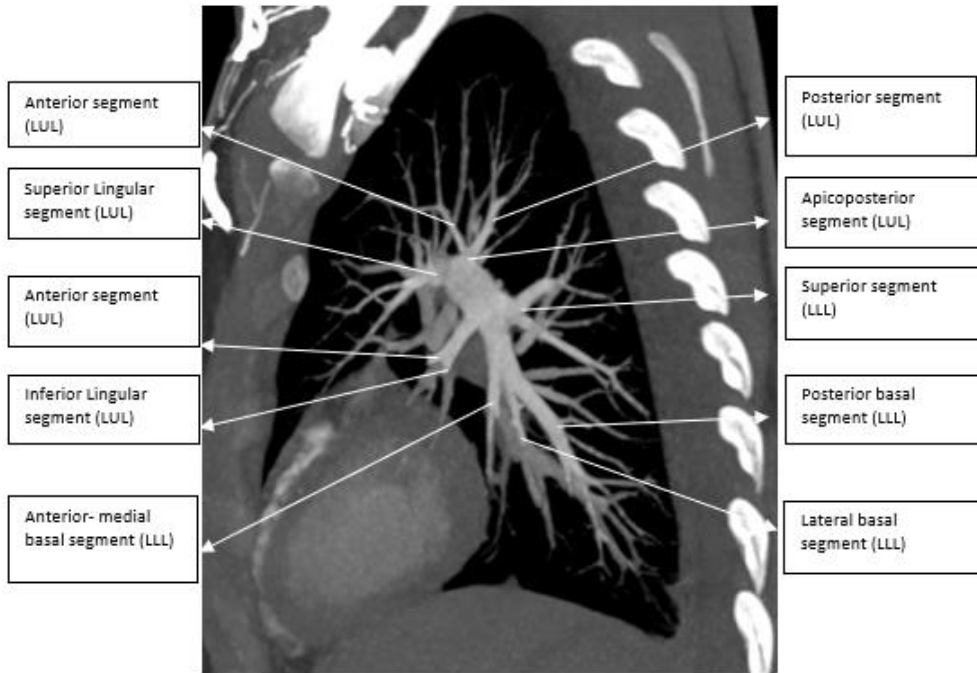


Figure 3: MIP image of CTPA showing branches of left pulmonary artery

Risk factors for pulmonary embolism

The cause of venous thromboembolism (VTE) is thought to be a combination of the risk factors specific to each patient and the environment or circumstances around the event. In contrast to the conditions, patient-associated risk factors are typically long-lasting. Age, a history of VTE, active cancer, or other incapacitating illnesses like heart failure or respiratory failure are all considered risk factors for patients. Hormone replacement medication and oral contraception are also risk factors. The British Thoracic Society states that risk factors have historically been divided into major and minor categories (Table 2). A population at risk for VTE is thought to include critically sick individuals getting intensive care (8).

TABLE 1: The mortality rate of acute pulmonary embolism according to Czech and European Guidelines

Clinical presentation of acute pulmonary embolism	Mortality rate
Unselected population	11.4% at two weeks 17.4% at three months
<u>Massive pulmonary embolism</u>	
Overall	18% to 65%
Treated	Approximately 20%
With cardiogenic shock	25% to 30%
With resuscitation	65%
Submassive pulmonary embolism	5% to 25%
Pulmonary embolism with mobile thrombi in right-heart chambers	As high as 27%
Small pulmonary embolism	Up to 1%

Table 2: Risk factors of venous thromboembolism, according to the British Thoracic Society, 2003

Major risk factors (RR = 5 to 20)	Minor risk factors (RR = 2 to 4)
<ul style="list-style-type: none"> • Postoperative states: Major abdominal/pelvic surgery, hip/knee joint replacement, postoperative intensive care • Obstetrics: Late pregnancy, Caesarean section, puerperium • Lower limb affections: Fractures, extensive varicosities • Malignancies: Abdominal/pelvic, advanced/ metastatic stage • Limited mobility: Hospitalization, geriatric care Miscellaneous: History of previous venous thromboembolism 	<ul style="list-style-type: none"> • Cardiovascular: Congenital heart disease, heart failure, hypertension, superficial venous thrombosis, central venous catheter • Humoral: Estrogen use: oral contraception, hormone replacement therapy • Miscellaneous: Chronic obstructive lung disease, neurological impairment, latent malignancy, thrombotic defects, long-distance travel in the sitting position, obesity • Other: Inflammatory bowel disease, nephrotic syndrome, chronic dialysis, myeloproliferative disease, paroxysmal nocturnal hemoglobinurias catheter

Medical history

More than 85% of patients with PE typically complain of rapid onset or worsening resting dyspnea as their primary complaint. PE can also manifest as progressive exercise-induced dyspnea, though. Additionally, more than 50% of patients report chest pain that might occasionally be difficult to distinguish from angina of ischemic etiology. PE pain is typically acute, stinging, and sometimes associated with respiratory excursions rather than being dull. Cough (around 20% of patients), hemoptysis (7%; a complication of lung infarction), and syncope (14%), among others, are additional PE manifestations. Dyspnea, chest discomfort, and hemoptysis—a frequently reported triad—do not truly happen frequently (5% to 7%). However, dyspnea, tachypnea, or chest discomfort are present in more than 90% of PE patients. PE can finally lead to cardiac arrest, shock, or hypotension in the most severe cases (see below). Patients with severe central PE who experience significant hemodynamic effects frequently experience isolated, rapidly increasing dyspnea. This is in contrast to small embolisms that block peripheral pulmonary artery branches and manifest as a lung infarction syndrome with few or no symptoms. (8)

Review of Literature

1. In a study titled "Role of dual-energy CT in diagnosis of Pulmonary Embolism," Shen et al. retrospectively analyzed the clinical data of 87 patients who had had DEPI between August 2017 and July 2018 at Jiaying Second Hospital and had been suspected of having a pulmonary embolism. A diagnostic test was conducted to determine the diagnostic coincidence rate, sensitivity, specificity, positive predictive value, negative predictive value, positive likelihood ratio, and negative likelihood ratio for the diagnosis of DEPI and CTPA using the results of CTPA as the reference standard and patients and pulmonary lobes, respectively, as evaluation units. Conclusions DEPI offers excellent sensitivity, specificity, and accuracy for detecting pulmonary embolism. The simultaneous acquisition of anatomical structural and functional information images by DEPI and CTPA significantly increases the diagnostic precision for pulmonary embolism. Therefore, the preferred evaluation for patients with clinically suspected pulmonary embolism can be employed. (9)

2. In a study, Dagmar Grob et al. compared DECT iodine maps to CT angiography for PE detection and subtraction CT for PE detection. Between July 2016 and April 2017, 274 patients thought to have PE had pre-contrast CT followed by contrast material-enhanced DECT angiography. Iodine maps were produced using DECT. After motion correction, subtraction maps (contrast-enhanced CT minus pre-contrast CT) were generated. Conclusion: Without the requirement for specialized hardware, Subtraction CT had a diagnostic performance comparable to DECT. (7)

3. In research to see if there is a benefit to employing DECT iodine maps and standard CT angiography images to identify pulmonary embolism, Elizabeth k. Wiedman et al. DECT iodine maps show modest additional improvements for diagnosing occlusive segmental and subsegmental pulmonary emboli, according to their analysis of 1144 patients. (10)

4. To determine whether quantitative dual DECT characteristics offer an incremental risk advantage over CT ventricular diameter ratio in patients with acute PE, Dong Jin Im et al. undertook a study. A study involving 480 patients concluded that CT ventricular diameter ratio, rather than the quantitative evaluation of lung perfusion defect volume by DECT, was the more accurate predictor of all-cause mortality within 30 days. (11)

5. In a research published in July 2014, S F Thieme et al. investigated the potential diagnostic utility of dual-energy CTPA's vascular and pulmonary parenchymal enhancement values. One thousand three hundred twenty-one patients and 142 control patients had their DE-derived pulmonary parenchymal, pulmonary artery, and left atrium enhancement values assessed. They concluded that individuals with congestive heart failure did not have altered perfused blood volume in DE-CTPA but that there were variations in enhancement values in the pre-and post-pulmonary arteries compared to the control group. (5)

6. Between July 2016 and April 2017, Dagmar Grob et al. studied the image quality of iodine maps derived from DECT and subtraction CT for pulmonary embolism. They included 55 patients with suspected PE in their investigation. They concluded that subtraction CT had a similar to higher signal-to-noise ratio and had better picture quality of pulmonary iodine maps than DECT. (12)

7. In march 2016, Mao X et al. carried out a study titled "Diagnostic Value of Dual-Source Computerized Tomography Combined with Perfusion Imaging for Peripheral Pulmonary Embolism" with the participation of 32 patients who had dual-source CT scans and were suspected of having pulmonary emboli.

They discovered that while PED scans showed 68 (10.63%) segmental and 94 (7.34%) sub-segmental pulmonary embolisms, CTPA images only revealed 50 (7.81%) segmental and 56 (4.38%) sub-segmental pulmonary embolisms. As a result, the CTPA images' detection rate for

peripheral pulmonary embolism was substantially lower than the PED images' (P 0.05). The diagnostic agreement of PED, CTPA, and DEPI for segmental pulmonary embolism was good (kappa = 0.85). For the diagnosis of pulmonary embolism, DEPI pictures had a sensitivity and specificity of 91.7% and 97.5%, respectively (1).

8. Palm V et al. studied Acute Pulmonary Embolism: Imaging Techniques, Findings, Endovascular Treatment, and Differential Diagnoses.

In addition to outlining crucial differential diagnoses for acute non-thrombotic PE and non-embolic pulmonary artery illness, this review examines imaging modalities, diagnostic algorithms, imaging findings, and endovascular therapy of acute thrombotic PE. The review emphasizes knowledge pertinent to ordinary radiological practice and draws attention to recent advancements that are easily applicable in clinical practice.

They concluded that the current reference standard for diagnosing acute PE is CTPA. Patients who are pregnant, young, have a contraindication to iodinated contrast, or who have other medical conditions should undergo ventilation and perfusion (VQ) scanning or magnetic resonance imaging (MRI) in centers with the necessary expertise. Only patients who will receive endovascular treatment should undergo invasive angiography. Always consider artifacts, acute non-thrombotic PE, chronic PE, and non-embolic pulmonary artery disorders as other diagnoses (3).

9. Value of DEPI using a Dual-source CT System for Pulmonary Embolism was the focus of a 2018 study by Zhang J et al.

The DEPI (lung perfusion and CTA images of the pulmonary artery acquired by the Dual Energy program) and emergent DSA angiography were offered to 50 patients with a high prevalence of acute PE (golden diagnostic criterion).

CTA was used to examine 1020 pulmonary segments and 260 pulmonary arteries. Embolisms were found in 50 lung lobes, 108 pulmonary segments, and 82 sub-segments. Through DEPI, reduction or lack of perfusion was discovered in 103 pulmonary segments, 78 subsegments, and 48 lung lobes (concordance rates of 96.0%, 95.4%, and 95.1%, respectively). The number of embolisms and the morphological features of the pulmonary artery between CTA images and DEPI images did not differ statistically from each other.

They concluded that using a dual-source CT system in conjunction with DEPI can improve application value in the detection of pulmonary embolism (2).

10. DECT for the Assessment of Contrast Material Distribution in the Pulmonary Parenchyma was the subject of a study by Thieme SF et al.

On a dual-source CT scanner, 93 patients received CT angiography using the dual-energy approach. Iodine in the lung parenchyma was mapped using post-processing based on its spectral behavior, and two readers judged the quality of the images. Iodine distribution patterns were classified as faults, whether uniform, patchy, or confined. The same data sets' conventional CT angiographic reconstructions were examined for the existence and localization of pulmonary embolism, the degree of embolic blockage, and alterations in the lung parenchyma. In per-patient and per-segment studies, the dual-energy perfusion results were associated with the CT angiographic and lung-window results.

They concluded that DECT is trustworthy in identifying pulmonary parenchymal iodine distribution abnormalities that correspond to embolic artery blockage.

A study was conducted by Ma G et al. on "Influence of Monoenergetic Images at Different Energy Levels in Dual-Energy Spectral CT on the Accuracy of Computer-Aided Detection for Pulmonary Embolism. They retrospectively assessed the CT scans of 20 PE patients with spectral CTPA. Using commercially accessible CAD software, nine sets of monochromatic

pictures with a 5 keV spacing between them were recreated and separately examined for the presence of PE. Two skilled radiologists reviewed all images and manually counted the emboli as the reference standard. To determine the number of true positives and false positives using CAD and to compute the sensitivity and false positive rate at various energies, the CAD findings for the number of PE at different energies were compared with the reference standard. True emboli numbered 120. At 40–80 keV, there were a total of 48, 67, 63, 87, 106, 115, 138, 157, and 226 CAD-detected PEs. High energies produced images with high sensitivities and low false positive rates, while low energies produced images with low sensitivities and high false positive rates. CAD attained the ideal combination of high sensitivity and the low false positive rate at 60 keV and 65 keV, where sensitivity was 81.67% and 84.17%, respectively, and false positive rate was 7.55% and 12.17%, respectively. They concluded that monochromatic images of various energies influence the accuracy of CAD for PE in dual-energy spectral CT. The best combination of high sensitivity and low false positive rate for identifying PE is achieved by combining CAD with pictures at 60–65 keV (13).

11. DECT blood volume evaluation in acute pulmonary embolism - connection with D-dimer level, right heart strain, and the clinical prognosis was the subject of a 2011 study by Bauer RW et al.

A retrospective analysis was performed on 53 individuals with acute PE who had DECT pulmonary angiography. On DE iodine maps, the pulmonary PD size brought on by PE was quantified both absolutely (VolPD) and relative to the overall lung capacity (RelPD). Right heart strain (RHS) symptoms were identified on a CT scan. Data were gathered on d-dimer levels, readmission for PE recurrence, and mortality.

Results showed a weak ($r = 0.43-0.47$) correlation between D-dimer level and PD size. In comparison to patients without RHS, patients with RHS had substantially higher VolPD (215

vs. 73 ml) and RelPD (9.9 vs. 2.9%) (p 0.003). In 18 patients with >5% RelPD, PE caused two fatalities and one readmission, whereas no such occurrences were discovered in patients with 5% RelPD.

They concluded that in this pilot trial, the pulmonary blood volume on DECT in acute PE correlates with RHS and appears to predict patient outcome (14).

12. Fink C et al. conducted a study in 2008 on DECT angiography of the lung in patients with suspected pulmonary embolism. In patients with suspected pulmonary embolism, determine whether dual-energy CT angiography (CTA) of the lung is feasible (PE). A single-acquisition, dual-energy CTA technique was used on 24 patients with suspected PE on a dual-source CT system (A-system: 140 kV/65 mAs ref, B-system: 80 kV/190 mAs ref). By employing specialized dual-energy post-processing software to color-coded voxels containing iodine and air, lung perfusion was made visible. Two blinded radiologists assigned perfusion deficiencies a PE consistency or non-PE consistency rating. Using a 5-point scale, perfusion maps and CTA's subjective image quality was appraised (1: excellent, 5: poor). The reference standard for the PE diagnosis was the reading of a third independent radiologist. Perfusion faults defined as consistent with PE were found in the afflicted lung regions in all individuals with PE (n = 4). In any of the patients without PE, neither reader found any perfusion deficits that were consistent with PE. Therefore, the sensitivity and specificity for the PE assessment were 100% for each patient for both readers. Sensitivity and specificity per segment varied between 60 and 66.7% and 99.5 and 99.8%. (K = 0.81) The interobserver agreement was favorable. The most common reason for perfusion problems graded as not consistent with PE was streak artifacts from dense contrast material in the great thoracic arteries. The perfusion maps and CTA had an average picture quality score of 2, which was 2.

As a result, dual-energy CTA of pulmonary embolism is practical and enables the evaluation of perfusion abnormalities brought on by pulmonary embolism. The injection protocol has to be improved further to reduce artifacts from dense contrast material (15).

13. A study entitled Impact of Iodine Delivery Rate with Varying Flow Rates on Image Quality in DECT of Patients with Suspected Pulmonary Embolism was carried out in 2013 by Hansmann J et al. A total of 120 patients were randomly assigned to different contrast material injection regimens with various iodine concentrations and iodine delivery rates (IDRs): Iopromide concentrations of 80 mL at 4 mL/sec result in IDR of 1.4 gI/sec; 80 mL at 3 mL/sec results in IDR of 1.1 gI/sec; 98 mL at 4.9 mL/sec results in IDR of 1.4 gI/sec; and 98 mL at 3.7 mL/sec results in IDR of 1.1 gI/sec. Subclavian vein-superior vena cava-right atrium, right ventricle-pulmonary trunk-pulmonary arteries, and outflow tract attenuation values were measured (left atrium-left ventricle-ascending aorta). Two readers evaluated the iodine perfusion maps and CTPA images for subjective image quality. The number of artifacts caused by hyperdense contrast material was counted on iodine perfusion maps.

Protocol A with 374 98 Hounsfield units (HU) (highly concentrated contrast material/high IDR) had the maximum target tract attenuation. When compared to procedures B and D, this was significant ($P = .0118$ and $P = .0427$, respectively), but not when compared to treatment C ($P = .3395$). The target tract attenuation for protocols B (309 80 HU), C (352 119 HU), and D (325 74 HU) did not differ significantly from one another. Compared to all other procedures, protocol A's CTPA and DEPI image quality received significantly superior ratings (median score = 5/4; $P = .0001$ for both), with only moderate interreader agreement ($k = 0.58/0.47$). Compared to protocols C and D, procedures A and B showed more artifacts on iodine perfusion maps (3 versus 2).

They concluded that, even though there are more artifacts on the DEPI maps, the diagnostic image quality is improved when highly concentrated iodinated contrast material is used in conjunction with high flow rates, which also has the highest target-tract attenuation for DE-CTPA protocols. (16)

Aims and objectives

Aim:

To evaluate the role of Dual-Energy CT (DECT) in the detection of pulmonary embolism.

Objective:

To assess the independent roles of CT Pulmonary Angiography (CTPA) and Dual- Energy Perfusion Imaging (DEPI) Maps in the detection of pulmonary embolism and to evaluate the additional advantage of DEPI maps.

Materials and methods

The study was carried out at the Department of Diagnostic and Interventional Radiology, AIIMS, Jodhpur.

Type of Study: Prospective observational study.

Imaging technique used

The dual-source CT scanner used in our study comprises two x-ray tubes and two corresponding detectors (7). The two acquisition systems are mounted on the rotating gantry with an angular offset of 90°. One detector (detector A) covers a FOV of 78 cm, and the other detector (detector B) is restricted to a FOV of 33 cm. Each detector has a corresponding tube, and both tubes can be operated independently with regard to their kilovoltage and milliamperage settings. All DE-CTPAs were performed on a dual-source CT system (Siemens Somatom Drive 128 x 2 slice Dual Source Scanner and Siemens Somatom Definition Flash 128 x 2 Slice Multi-Detector CT Scanner). The non-ionic iodinated contrast material iohexol (contrapaque) 300mg/ml was injected through an 18 gauge intravenous canula in the right antecubital vein.

Forty ml of pure contrast material (300 mgI/ml) was injected with a flow rate of 4.5 ml/sec, followed by 20 ml of contrast mixed with 20 ml saline (to reduce the artifact caused by high-density contrast material into the subclavian vein and superior vena cava) with the same flow rate.

The examination was started using a bolus-tracking technique with a threshold of 100 HU in the superior vena cava with a scan time delay of 8 seconds. The caudocranial acquisition was chosen. A combination of a tin-filtered (Sn) 140-kVp and 100-kVp spectrum was used. Pitch was 0.6 sec at a rotation time of 0.28 seconds. Patients were taught to hold their breath when the scan was activated at the end of inspiration.

Image interpretation

1. Presence of pulmonary embolism, location (Right upper, right middle, etc.), size (central, segmental, subsegmental,) and type (occlusive and non-occlusive) of pulmonary embolism on CTPA.
2. Presence and types of defects (artifacts, consolidation, peripheral wedge-consistent with pulmonary embolism) on iodine map. Because the lung parenchyma also impacted the iodine map, the iodine perfusion defects were compared with the lung CT.
3. Correlated CTPA and iodine maps findings
 - a) Do pulmonary embolisms seen on CTPA?
 - b) Are there iodine map findings suspicious for pulmonary embolism?
 - c) Do they correspond to pulmonary embolism seen on CTPA?
4. Using Qanadli scoring, the CT obstruction index (CTOI) was also calculated (17). A total 10 segmental pulmonary arteries were thought to make up each lung's pulmonary artery tree: three for the upper lobes, two for the middle lobe or lingula, and five for the lower lobes. Emboli in segmental PAs were given a score of 1, and the number of segmental PAs

originating distally was used to assign a value to emboli at the most proximal artery level. Weighting factors were applied to each result (0 = no defect, 1 = partial occlusion, and 2 = complete occlusion) in order to provide further details on residual perfusion distal to the embolus. An isolated subsegmental embolus was given a value of 1 and a maximum CTOI of 40. It was regarded as a partially occluded segmental PA.

Study population:

Inclusion Criteria

All patients with a clinical suspicion of acute and chronic pulmonary embolism.

Exclusion Criteria

- Non-consenting patients.
- Pregnancy
- Patients who are not willing to participate in the study.

Study duration: One and a half years.

Sample size: All patients presenting with clinical suspicion of pulmonary embolism -acute and chronic within the time-bound span of 1.5 years, i.e., between January 2021 to June 2022, were imaged using dual-energy CTPA protocol (group 1).

The data of patients done by single energy CTOPA protocol during the previous one year were taken as control (group 2).

CT machine: All DE-CTPAs were performed on a dual-source CT system (Siemens Somatom Drive 128 x 2 slice Dual Source Scanner and Siemens Somatom Definition Flash 128 x 2 Slice Multi-Detector CT Scanner)

Dual-energy CT

The distinction and classification of various types of tissues are exceedingly difficult since the same CT values can represent materials with varied elemental compositions. In DECT, attenuation data at a second energy allow a mixture of two or three materials to be broken down into its component constituents.

Several technical methods for collecting dual-energy data include quick tube potential switching, multilayer detectors, sequential acquisition of two separate scans, and dual x-ray sources. (18)

Dual X-Ray Sources

Two x-ray sources and two data acquisition systems are mounted on the same gantry and placed orthogonally in a dual-source CT system (Fig 4). Siemens Healthcare debuted its first dual-source scanner, the Somatom Definition DS, in 2006; its second, the Somatom Definition Flash; and its third, the Somatom Force, in 2013. (Forchheim, Germany).

We have used the dual-source CT systems, Siemens Somatom Drive 128 x 2 slice Dual Source Scanner and Siemens Somatom Definition Flash 128 x 2 Slice Multi-Detector CT Scanner.

Each x-ray source has a separate high-voltage generator, allowing for independent control of the tube current and potential. The projected statistics are roughly 90 degrees out of phase. Material decomposition analyses are carried out in the image domain using the images reconstructed from each tube detector pair.

The noise levels in the corresponding photos can be altered because each tube is run at a different tube potential and various tube current values. When two tubes are concurrently activated, the detector for one tube may pick up dispersed radiation whose initial photon originated from the other tube and vice versa. Due to the degradation of spectral separation, a

suitable scatter-correction technique must be used. The ability to independently tailor the spectrum filtration for each tube-detector combination is a benefit of the dual-source technique, allowing for increased spectral separation and a higher signal-to-noise ratio in the material-specific pictures.

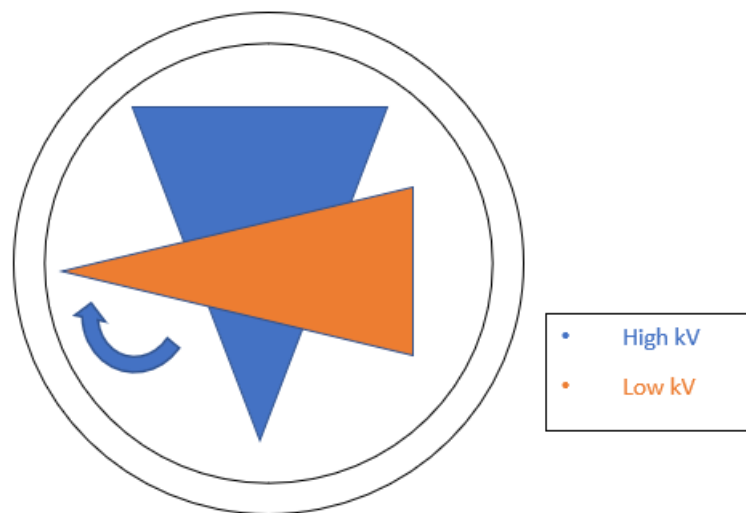


Figure 4: Dual-x-ray-source geometry: Dual-energy data can be collected simultaneously using separate x-ray tubes, detectors, and generators.

The best spectrum filtration and tube current setting can be used to operate each tube. Since the low and high-energy perspectives are 90 degrees apart, dual-energy processing utilizes already reconstructed image data. The temporal resolution is unaffected, and both axial and spiral acquisition modes are available. The orthogonal detector may pick up scatter from a single tube, reducing the need for spectral separation. Depending on the particular scanner model, the range of view over which dual-energy data can currently be captured is restricted to 26, 33, or 35 cm. Kilovoltage is denoted by kV.

Applications of Dual Energy CT in pulmonary embolism

Virtual Monoenergetic Imaging

Along with material-specific data, DECT also allows for creating monoenergetic images at various energies, which can be used for routine diagnosis in a manner comparable to traditional polyenergetic images obtained at a single x-ray tube potential. Even when image-based techniques are applied, these images reduce beam-hardening artifacts. Iodine signal increases for photon energies just above 33 keV due to the rapid increase in iodine attenuation above this energy. Patient size and the employment of energy-domain noise reduction techniques to address the increase in noise that would otherwise happen at lower energy settings are two aspects that affect the ideal energy at which to synthesize the virtual monoenergetic image. Iodine exhibits the best contrast-to-noise ratio at virtual monoenergetic energies between 40 and 70 keV. (18) Since the K- edge (keV) of iodine is 33.2, the attenuation of the enhanced structures containing iodine will be more at 100 keV as compared to 140 keV (Fig. 5A and Fig. 5B).

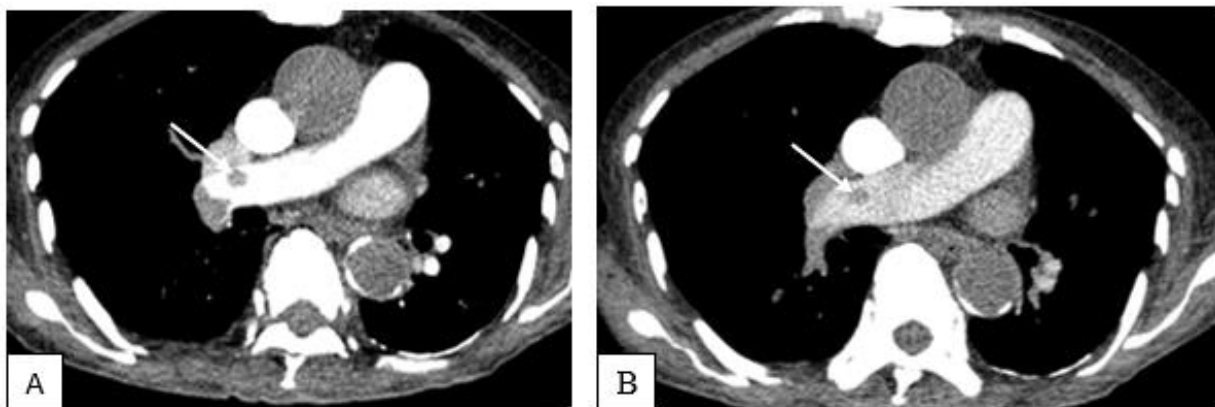


Fig. 5 A: Monoenergetic image at 100 keV – Better visualisation of thrombus (arrow) in right main pulmonary artery. Fig. 5 B: Monoenergetic image at 140 keV – Less-sharper image as compared to figure A with appreciation of thrombus (arrow) is more difficult.

Perfused Blood Volume (Blood Pool Imaging)

Identifying iodine voxels enables color enhancement of iodinated areas and bone removal to see iodine. One clinical application is visualizing the perfused blood volume, commonly known as blood pool imaging. Applications have been created to identify myocardial ischemia and locations of pulmonary embolism-related lung perfusion deficiencies. (18)

Virtual Non-contrast-enhanced Images

To construct a virtual non-contrast image or an image without the addition of contrast material, the iodine component of the CT number can be removed after iodine voxels have been identified. The non-contrast scan of multiphase exams can be unnecessary if the virtual non-contrast photos are good enough to stand in for real non-contrast images. (18)

Diagnostic Pitfalls of DECT

To prevent misdiagnosis, practitioners must be aware of the diagnostic hazards of DEPI imaging. An iodine map of the lung parenchyma has a high level of inter-reader agreement and enables quick diagnosis of perfusion abnormalities. Iodine maps selectively show iodinated contrast material inside the lung parenchyma, not real perfusion; hence they should be evaluated carefully. Additionally, PE does not necessarily result in iodine map perfusion abnormalities. While non-occlusive PE perfusion defects can occur at rates as low as 6-9% and other lung disorders can also result in perfusion defects, the rate of perfusion abnormalities on PBV for occlusive PE is rather high (82–95%). Streaky and beam-hardening effects around the rib, metallic objects, and around the high-concentration contrast agent in arteries bring about false perfusion defects in an iodine map. (4)

Perfusion defects can also be seen from non-PE causes, such as in cases of abnormal pulmonary vascular supply, artefactual perfusion defects, such as those in the lingual or right middle lobe (from cardiac pulsations), bilateral lower lobes close to the diaphragm (from respiratory motion), and streak and beam hardening artifacts from high-density contrast material streak in superior vena cava, subclavian artery, thoracic veins, and right In parenchymal problems such consolidation, atelectasis, emphysema, or tumors entering or squeezing pulmonary arteries, perfusion deficiencies are also seen. (4) Fig. 6 below shows artifacts in DECT.

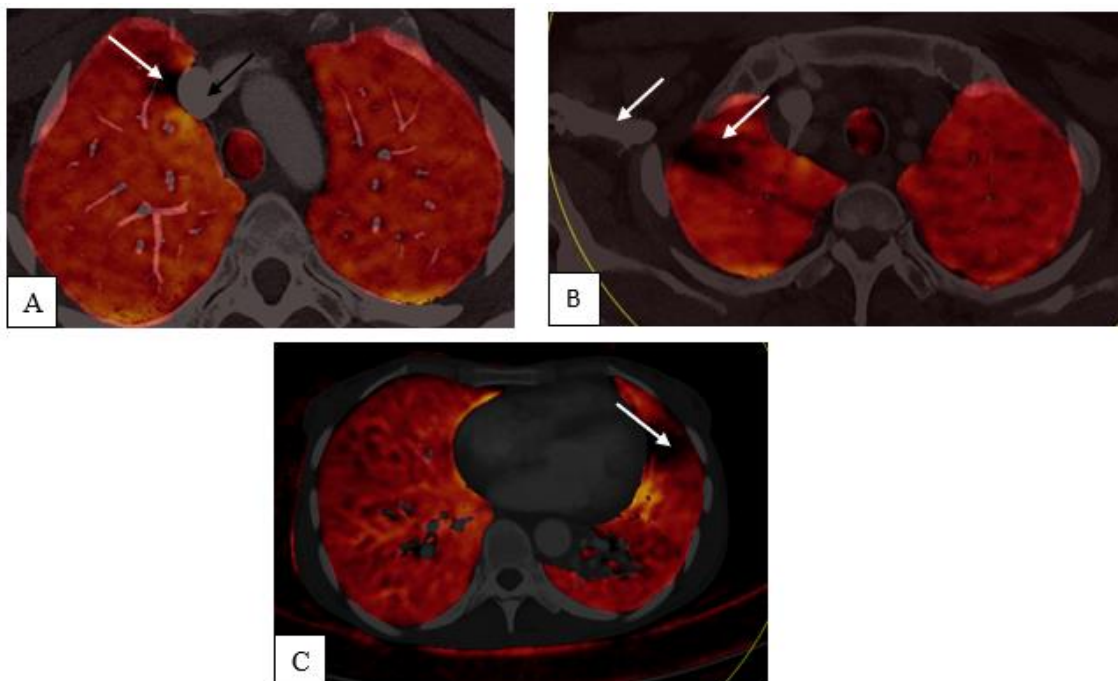


Fig: 6A- DEPI showing perfusion defect in right upper lobe (white arrow) due to high density contrast in superior vena cava (arrow)- beam hardening artefact.

6B- DEPI showing perfusion defect in right upper lobe (black arrow) due to high density contrast in right subclavian vein (white arrow)- beam hardening artefact.

6C- DEPI showing perfusion defect in lingular segment of left upper lobe (white arrow) due to cardiac pulsation.

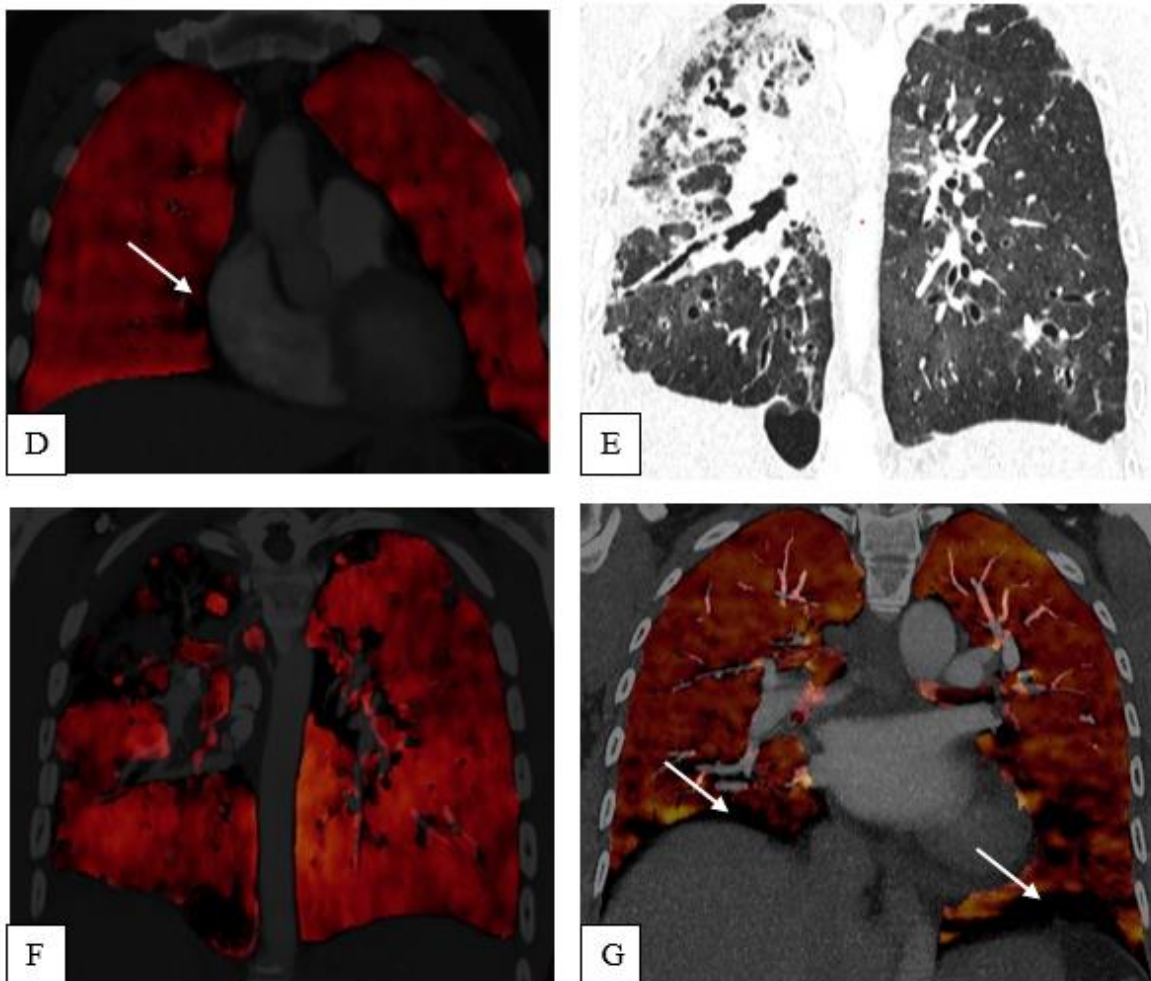


Fig: 6D- DEPI showing perfusion defect in right middle lobe (arrow) due to cardiac pulsation.

Coronal section of computed tomography, lung window (6E) showing abnormal parenchyma which is reflected as perfusion defects in DEPI in 6F.

6G- shows perfusion artefacts in bilateral lower lobes due to diaphragm movement.

CT angiographic findings of acute and chronic pulmonary embolism

Direct Signs of Acute PE

Complete Obstruction

A concave filling defect, often known as a "trailing edge," should be visible inside the contrast material at the level of the obstruction on pulmonary angiograms as the diagnostic evidence of acute PE with total obstruction. Catheter angiography cannot detect a thrombus distal to the obstruction, but a CT scan can detect it. Due to the thrombus being impacted by pulsatile flow at the thrombus location, the pulmonary artery diameter may increase. (19)

Non-obstructive Filling Defect

The location of a non-obstructive filling defect might be either central or eccentric. A central filling defect on angiography is entirely encircled by contrast material. On a CT scan, this finding appears as a clearly defined central filling defect in either the vessel's axial (polomint sign) or longitudinal (railroad track sign) planes.

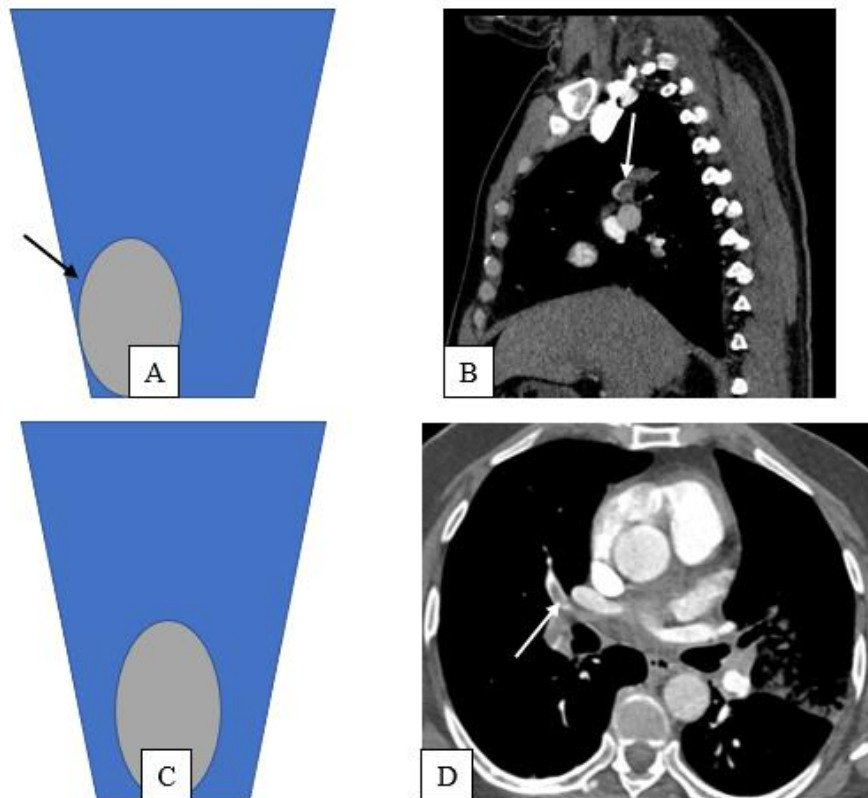
A nonobstructive central filling defect will be linked to either a nonobstructive eccentric filling defect or the thrombus of total obstruction since it is physically impossible to float within the lumen's center without physically touching the vessel wall. When detected on angiography or CT, a non-obstructive eccentric filling defect in acute PE forms sharp angles with respect to the artery wall. (19)

Indirect Sign of Acute Thromboembolic Disease

Differential Arterial Perfusion Angiograms frequently show oligemia, or a reduction in flow rate, as a result of acute PE. In our experience, angiography more frequently shows this finding than CT. A mosaic attenuation pattern on CT is a rare manifestation of nonuniform arterial perfusion brought on by acute PE. Occasionally, a significant acute central PE might result in

oligemia and a reversible decrease in vessel diameter seen on CT. The congenital or acquired causes of chronic PE, emphysema, infection, compression or invasion of a pulmonary artery, atelectasis, pleuritis, and pulmonary venous hypertension are included in the differential diagnosis of the indirect radiologic sign of nonuniform pulmonary arterial perfusion. (19)

Fig. 7 shows signs of acute pulmonary thromboembolism.

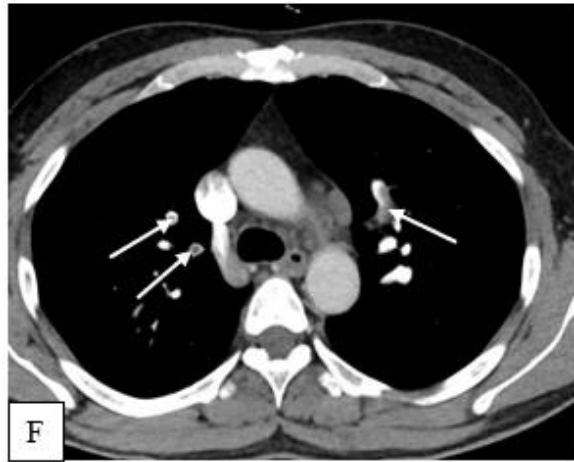
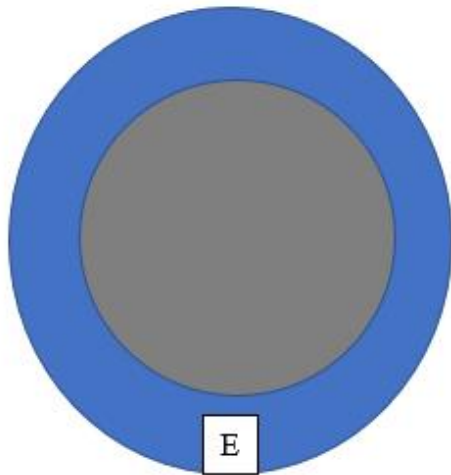


7 A. Illustration demonstrating the sharp angles that an eccentric acute thrombus (arrow) makes with the vessel wall.

7 B. Sagittal monoenergetic CTPA image showing acute thromboembolism with thrombus forming acute angle (arrow) with vessel wall

7 C. An illustration of an acute PE central filling defect on a CT scan showing the thrombus in long axis. Contrast is seen on either side of the clearly defined thrombus forming the "railroad track sign."

7 D. Axial monoenergetic CTPA image showing "railroad track sign" (arrow).



7 E- Well-defined central thrombus is completely surrounded by contrast material in the illustration of an acute PE central filling defect on a CT image that is being viewed perpendicular to the plane of the thrombus (the "Polomint sign")

7 F- Acute thrombi (arrows) in segmental branches of pulmonary arteries in bilateral lower lobes with right lower lobe segmental branches showing "Polomint sign"

7 G- Magnified view of right lower lobe segmental branches showing "Polomint sign" (arrows).

Direct Signs of Chronic PE

Complete Obstruction

Complete vascular cut-off caused by chronic embolism has been referred to as a "pouch" defect on angiography because it has a convex margin relative to the contrast material. This is different from how an obstruction would seem if an acute PE were to form obtuse angles with the vessel wall either unilaterally or bilaterally. Plaques resulting from pulmonary hypertension may potentially be the cause of pulmonary artery intimal abnormalities. (19)

Bands and Webs

A band is described as a fragile ribbon-like structure with free, unattached ends that is anchored to the vessel wall at both ends. A band typically has dimensions of less than 0.1 cm to 0.3 cm in width and 0.3 to 2 cm in length. It frequently faces the long axis of the vessel in the direction of blood flow. Bands with branches forming networks of varying complexity are called webs. On an angiography or CT scan, bands and webs appear as thin lines encircled by contrast material. (19)

Abrupt Vessel Narrowing

An abrupt convergence of contrast material leading to a thin column of intravascular contrast material distally is how abrupt vessel narrowing, which is frequently the result of recanalization, appears angiographically. The cause of the stenosis can be determined with CT scans, which also show this irreversible result. (19)

Indirect Signs of Chronic Thromboembolic Disease

Post stenotic Dilatation

A common sign of persistent thromboembolic illness is post-stenotic dilatation or aneurysm. Congenital and acquired causes, such as Marfan syndrome, are part of the differential

diagnosis. Mycotic aneurysms originating from septic emboli or nearby pulmonary infection, pseudoaneurysms brought on by extra- or endovascular trauma (such as pulmonary artery catheterization), Behçet disease, and Takayasu's arteritis are examples of acquired causes. (19)

Tortuous Vessels

Patients with pulmonary artery hypertension have been well-described as having tense pulmonary arteries. Additionally, patients with pulmonary artery hypertension brought on by chronic thromboembolic illness have this radiologic symptom. (19)

Enlargement of the Main Pulmonary Artery

Patients with precapillary, capillary, and post-capillary causes of pulmonary arterial hypertension experience enlargement of the main pulmonary artery greater than 33 mm. Patients with pulmonary artery hypertension brought on by persistent thromboembolic illness frequently have this radiologic finding. (19)

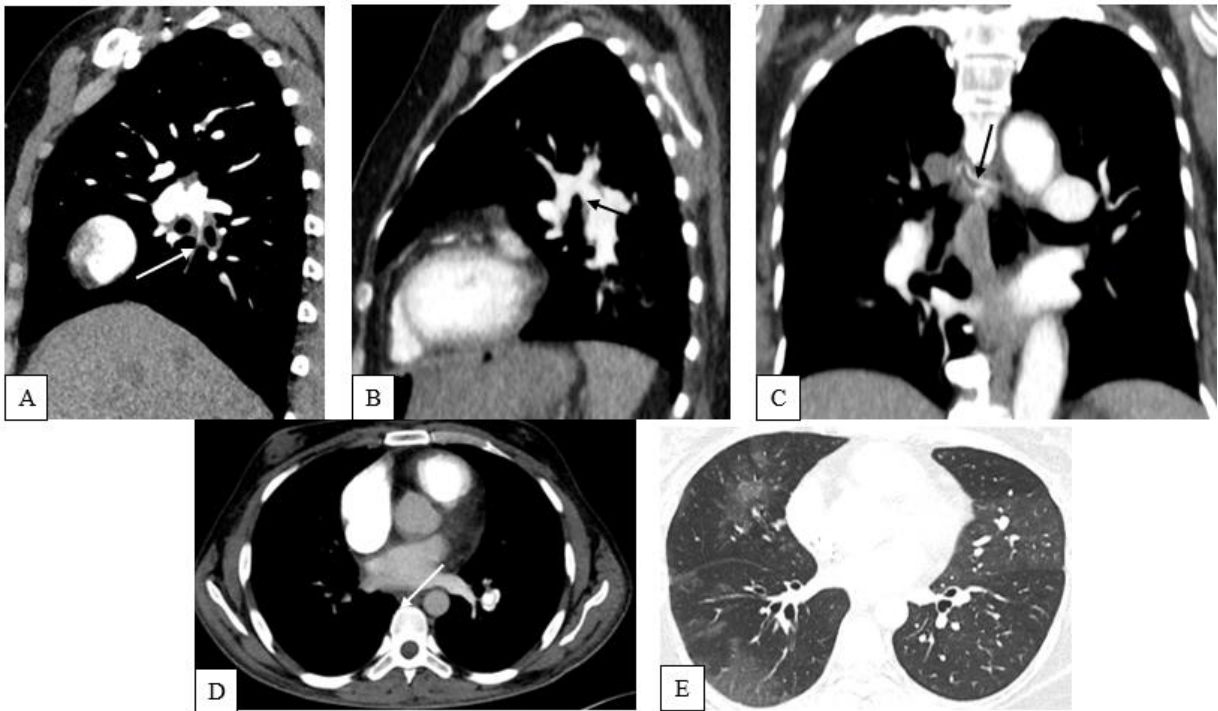
Enlargement of Bronchial Arteries

A common finding in patients with the persistent thromboembolic disease is enlarged bronchial arteries. Congenital vascular abnormalities, bronchiectasis, acute or chronic lung abscesses, and mycobacterial and fungal infections are additional reasons for this condition. However, standard pulmonary artery angiography cannot detect enlargement of the bronchial artery collateral supply. (19)

Nonuniform Arterial Perfusion

Chronic PE can result in an angiographically detectable nonuniform arterial perfusion pattern and show up as a mosaic pattern of lung attenuation on a CT scan. (19)

Fig 8 shows signs of chronic pulmonary thromboembolism.



8 A- CTPA imaging shows eccentric thrombus (arrow) causing abrupt vessel narrowing- known as "pruning".

8 B- CTPA imaging shows eccentric thrombus making obtuse angle (arrow) with the vessel wall.

8 C- CTPA MIP imaging showing enlarged and tortuous left bronchial artery (arrow).

8 D- CTPA imaging showing "web" like thrombus (arrow) in left lower lobe pulmonary artery.

8 E- High resolution computed tomography chest showing mosaic perfusion in a patient with chronic pulmonary thromboembolism.

Data Collection

Patient demographics, including age, gender, clinical history, any previous history of pulmonary thromboembolism, deep venous thrombosis, any known procoagulant state, prolonged travel, and any post-pregnancy status/ history of oral contraceptive pill intake, were recorded.

Investigations, including D-dimer and Electrocardiography (ECG), were also recorded.

The CTPA and DEPI maps were generated and studied in conjugation and separately for evaluation of pulmonary thromboembolism.

Statistical analysis

Data collected during the study was compiled using a Microsoft Excel spreadsheet and analyzed statistically using the statistical package for the MedCalc statistical Software version 20.115 for window editions. Qualitative data were presented as numbers and percentages, and qualitative data were presented as mean +SD and median. Comparison between groups was made by Chi-square test and unpaired test. A p-value less than 0.05 was considered to be statistically significant.

RESULTS

During the tenure of the thesis, patients with suspected pulmonary embolism were scanned using a dual-source CT system (Siemens Somatom Drive 128 x 2 slice Dual Source Scanner and Siemens Somatom Definition Flash 128 x 2 Slice Multi-Detector CT Scanner). Seventy-three patients were scanned and analyzed using the DECT protocol for pulmonary angiography and assigned as group 1. Seventy-seven patients who were scanned using the single-energy CTPA protocol in the previous one year were assigned as group 2 for comparison.

TABLE 3:

Age (years)	Group 1(using DECT protocol)		Group 2(using single energy CTPS protocol)	
	N	%	N	%
≤20	2	2.74	8	10.39
21-30	6	8.22	12	15.58
31-40	14	19.18	7	9.09
41-50	12	16.44	13	16.88
51-60	15	20.55	21	27.27
≥61	24	32.88	16	20.78
Median	53		50	
Range	10-97		14-82	
Mean ± SD	51.47 ± 17.14		46.42 ± 17.78	
t & p-value	1.769, 0.078			

In this study, the subjects lie in the age group of 10-97 years. The number of subjects in the age group ≤ 20 years is 2 (2.74%) in group 1 and 8 (10.39%) in group 2 ; 21-30 years age group is 6 (8.22%) in group 1 and 12 (15.58%) in group 2 ; 31-40 years age group are 14 (19.18%) in group 1 and 7 (9.09%) in group 2 ; 41-50 years age group are 12 (16.44%) in group 1 and 13 (16.88%) in Group 2 ; 51-60 years age group are 15 (20.55%) in group 1 and 21 (27.27%) in group 2 and ≥61 years age group are 24 (32.88%) in group 1 and 16 (20.78%) in group 2. The data comparison between the two groups was statistically not significant.

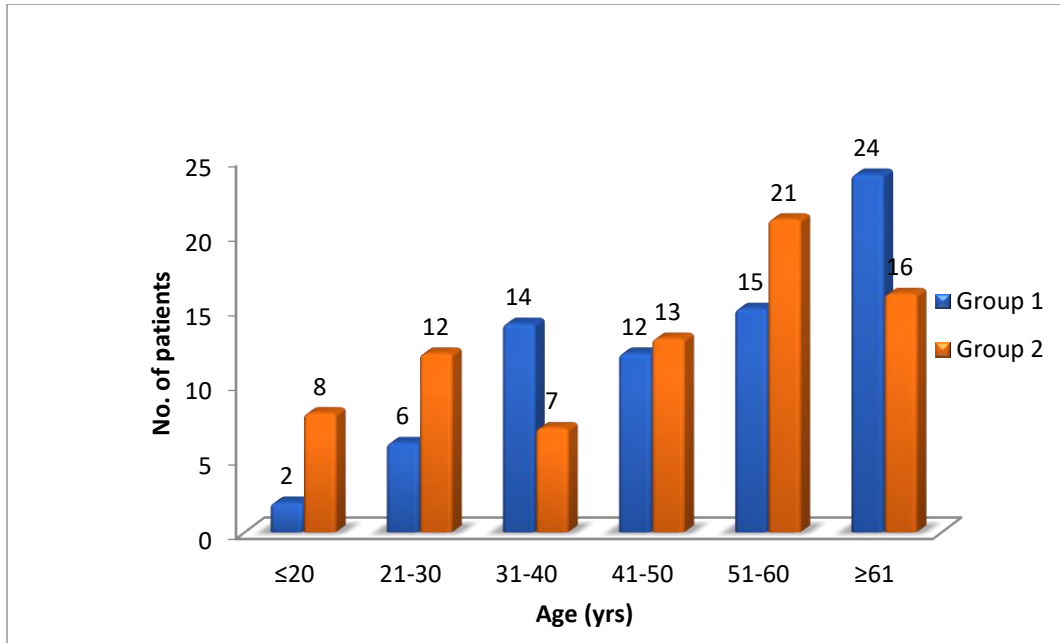


Fig. 9 Shows a bar graph with age-wise case distribution in two study groups.

TABLE 4:

Gender	Group 1		Group 2	
	N	%	N	%
Male	48	65.75	46	59.74
Female	25	34.25	31	40.26
Total	73	100.00	77	100.00

Chi-square 0.579, P value 0.446 (NS- not significant)

In this study, the numbers of males in group 1 are 48 (65.75%), group 2 is 46 (59.74%), and females cases in group 1 are 25 (34.25) and group 2 are 31 (40.26%). The data comparison between the two groups was not statistically significant.

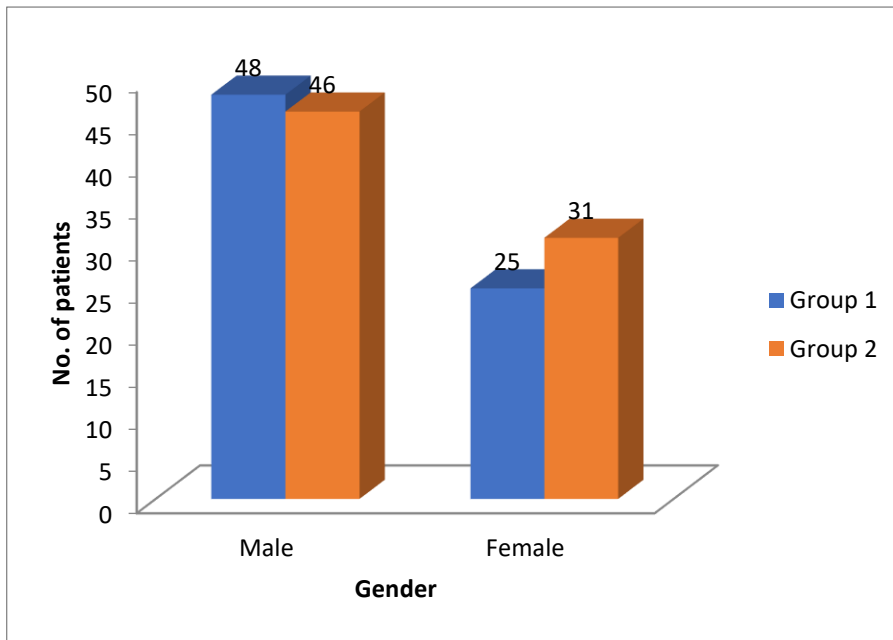


Fig. 10: Bar graph showing gender distribution of cases in 2 groups of study.

TABLE 5:

Pulmonary embolism	Group 1		Group 2	
	N	%	N	%
Present	21	28.77	20	25.97
Absent	52	71.23	57	74.03
Total	73	100.00	77	100.00

Chi-square 0.147, P value 0.701 (NS)

In this study, pulmonary embolism were present in 21 (28.77%) patients in group 1 and 20 (25.97%) patients in group B. The data comparison between the two groups was not statistically significant.

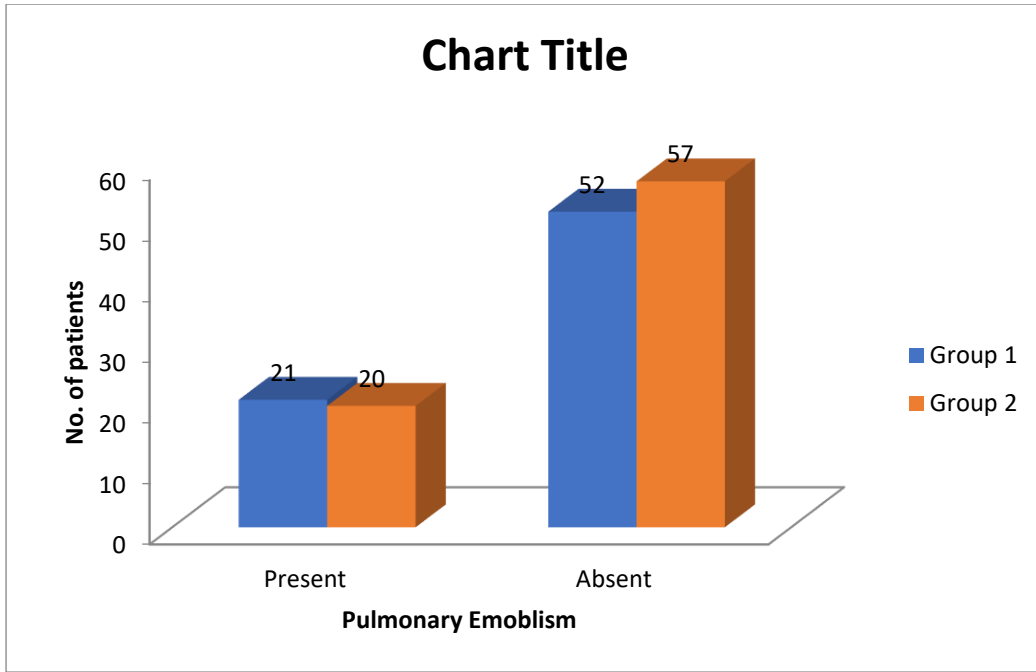


Fig.11: Bar graph showing the status of pulmonary embolism in 2 groups of the study

TABLE 6:

	Radiation dose (mSV)			
	Mean	Std	Median	Range
Group 1	1.59	0.58	1.42	0.90-3.60
Group 2	1.06	0.70	0.87	0.25-4.10

P value: < 0.0001

In this study, the mean radiation dose in group 1 is 1.59mSV, and in group B is 1.06mSV.

This data is expressed in bar chart form in Fig. 13. The radiation exposure in the DECT group was significantly higher than single energy comparison group. However, the radiation dose was lesser than the previous studies.

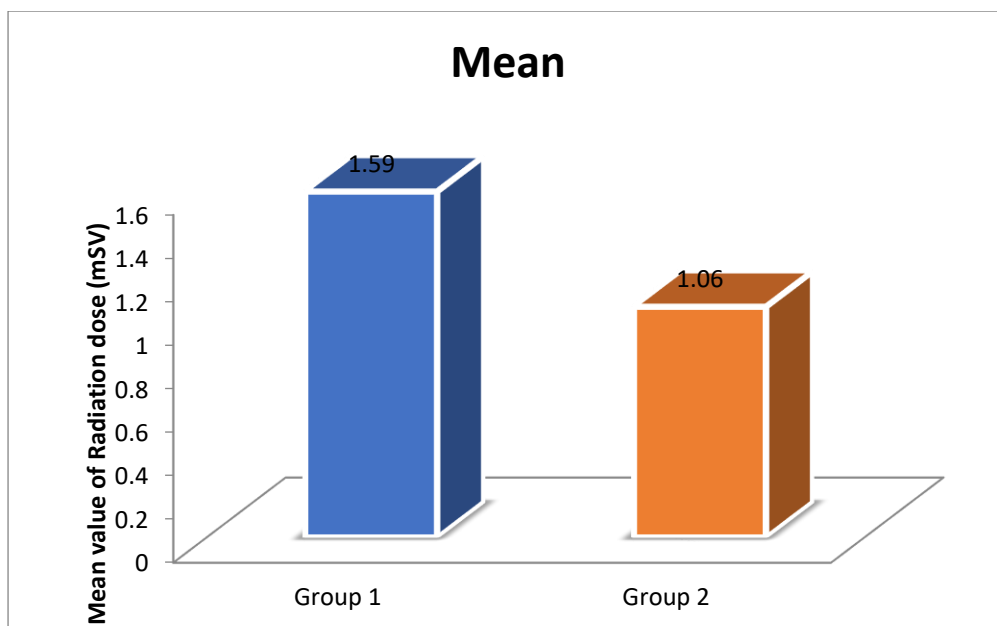


Fig. 12: Bar graph showing radiation dose in 2 groups of study

TABLE 7:

D-Dimer	Pulmonary Embolism				Total	
	Present		Absent			
	N	%	N	%	N	%
Increase	23	92.00	52	83.87	75	86.21
Normal	2	8.00	10	16.13	12	13.79
Total	25	100.00	62	100.00	87	100.00

P value 0.495 (NS)

Sensitivity - 92%
 Specificity - 16.13%
 PPV - 30.67%
 NPV - 83.33%
 Diagnostic Accuracy - 37.93%

The sensitivity of D-dimer in the prediction of pulmonary embolism is high (92 %), according to the study, but specificity is low (16.13 %). PPV and NPV of D-dimer in predicting pulmonary embolism are 30.67 % and 83.33 %, respectively.

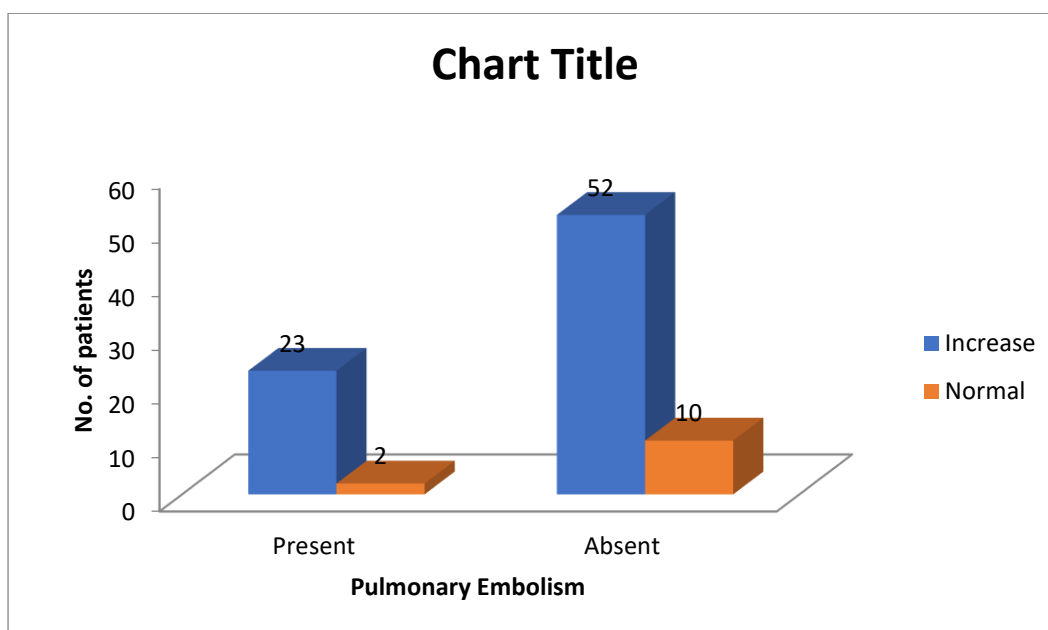


Fig. 13: Bar graph showing the correlation of D- dimer and status of pulmonary embolism

We have examined all the 72 patients scanned in dual-energy and found that 13 patients had acute pulmonary thromboembolism and seven patients had chronic pulmonary thromboembolism.

TABLE 8:

Age (years)	Acute		Chronic	
	N	%	N	%
21-30	1	7.69	1	14.29
31-40	4	30.77	0	0.00
41-50	1	7.69	1	14.29
51-60	1	7.69	4	57.14
≥61	6	46.15	1	14.29
Median	60		54	
Range	27-97		23-75	
Mean±SD	54.76±19.52		52.85±15.48	

t & p-value

0.223, 0.825

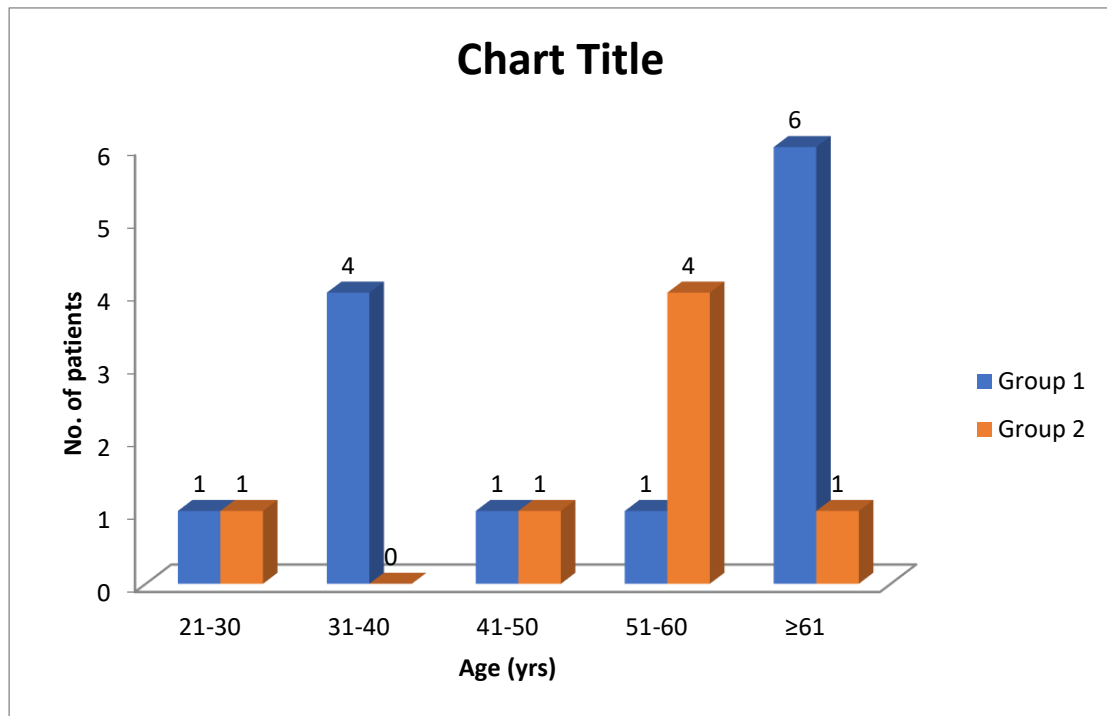


Fig. 14: Bar graph showing the age-wise distribution of patients with acute and chronic thromboembolism scanned in dual-energy protocol

In this study, the number of subjects with acute pulmonary thromboembolism lies in the age group of 27-97 years, and chronic pulmonary thromboembolism lies in the age group of 23-75 years. The maximum number of patients, six (46.15%) with acute pulmonary thromboembolism, were seen in 51-60 years age group.

The maximum number of patients, four (57.14%) with chronic pulmonary thromboembolism, were seen in >60 years age group.

Acute pulmonary thromboembolism

TABLE 9: Acute pulmonary thromboembolism

Site of thrombus	Number of thrombi	Percentage
Central	11	8.40
Segmental	39	29.77
Subsegmental	14	10.69
Segmental +Subsegmental	66	50.38
Central extending into segmental & subsegmental	1	0.76
Total	131	100

Out 13 patients with acute pulmonary thromboembolism, we found total 131 pulmonary thrombi. Out of which 11 (8.4 %) thrombi were located at central level, 39 (29.77 %) thrombi were located at the segmental level, 14 (10.69 %) thrombi were located at subsegmental level, 66 (29.77 %) thrombi were located at segmental level extending into subsegmental pulmonary arteries and 1 (0.76 %) thrombus was located at central level extending into segmental and subsegmental pulmonary arteries.

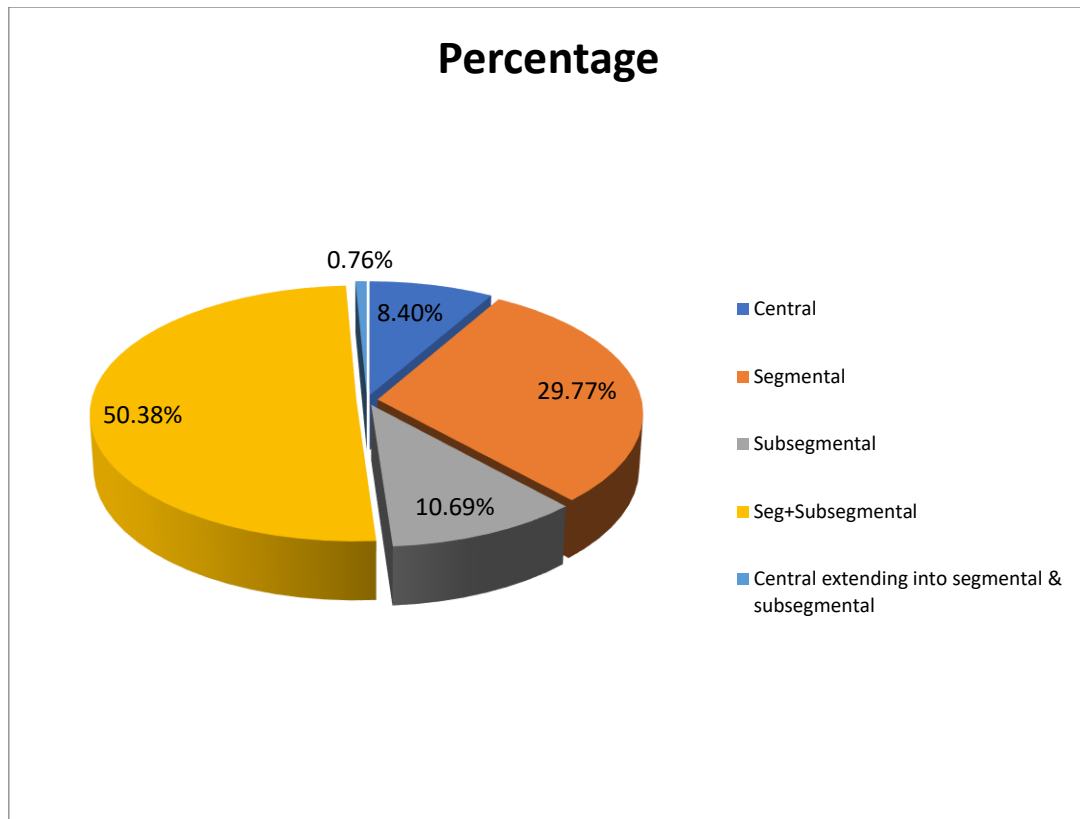


Fig. 15: Pie chart showing the proportion of various sites of thrombotic occlusion in patients with acute pulmonary embolism scanned in dual-energy protocol

TABLE 10: Acute pulmonary thromboembolism

Site of thrombus	No. of patients (after excluding two patients)	No. of perfusion defect	Perfusion defect %
Central	10	0	0.00
Segmental	22	5	22.7
Subsegmental	14	11	78.5
Segmental +Subsegmental	62	49	79
Central extending into segmental & subsegmental	1	1	100.00
Total	109	66	60.55

In all the patients with acute pulmonary thromboembolism, we looked for thrombus. We correlated the finding with DEPI maps to determine whether that thrombus was causing perfusion defect on DEPI maps. Thrombus which cause perfusion defect on DEPI maps are completely occluding thrombus, and thrombus which does not cause any perfusion defect on iodine map are either non-occluding or partially occluding thrombus.

Out of 13 patients with acute pulmonary thromboembolism, we have excluded two patients from the evaluation of DEPI maps due to either technical issues in generating DEPI maps or significant associated lung parenchymal abnormality interfering with perfusion assessment.

After excluding two patients out of 13, the total thrombi seen were 109, and iodine perfusion defects were seen in 66 (60.55%) thrombi. The iodine perfusion defects were seen in zero out of 10 in central thrombi; 5 out of 22 (22.7 %) in segmental thrombi; 11 out of 14 (78.5 %) in subsegmental thrombi, 49 out of 62 (79 %) in segmental thrombi extending into subsegmental arteries; and one out of one in central thrombi extending into segmental & subsegmental arteries.

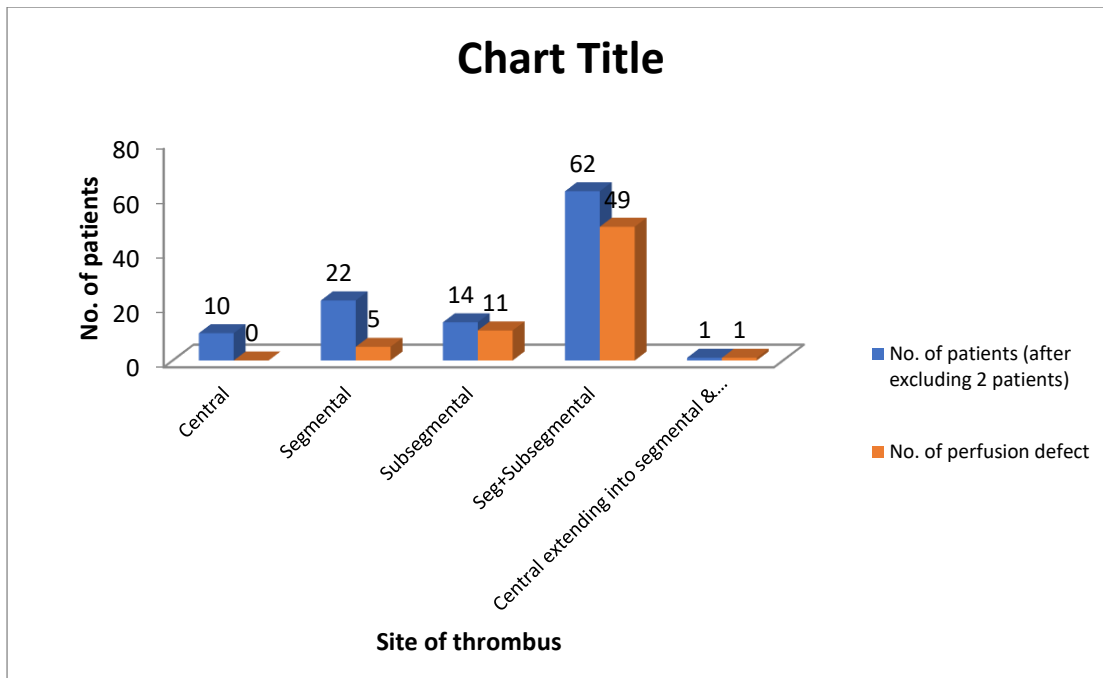


Fig. 16: Bar graph showing the proportion of patients with acute pulmonary embolism with various sites of thrombotic occlusion showing perfusion defect on DEPI maps.

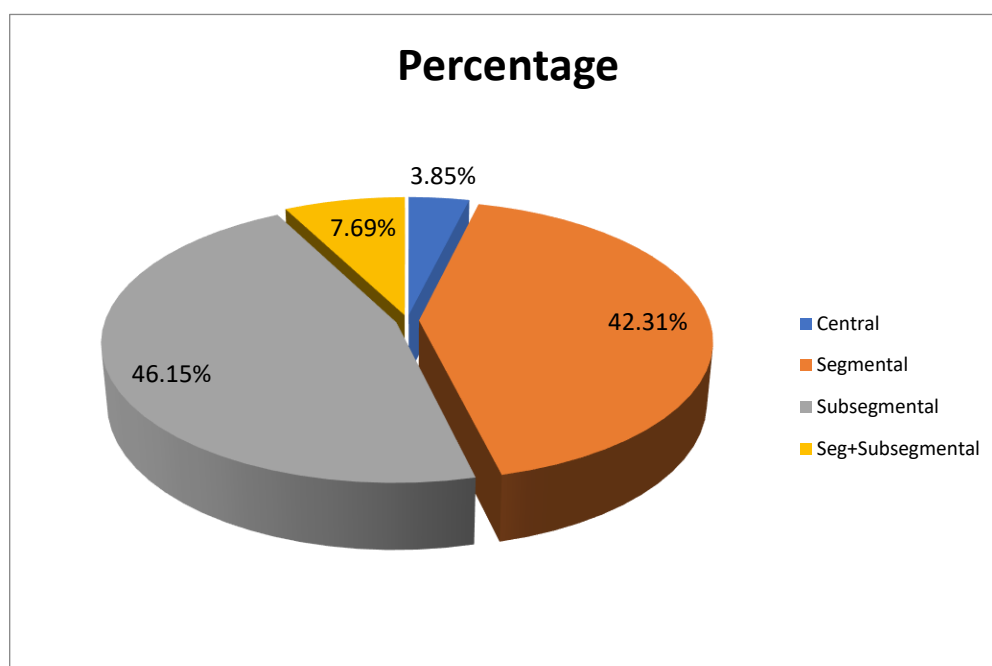
Two out of 11 patients with acute pulmonary thromboembolism, it was difficult to see the thrombus by monoenergetic CTPA because it was present at subsegmental level. However, the perfusion defects were seen on DEPI maps, and by retrospectively examining CTPA, thrombus were diagnosed confidently.

Chronic pulmonary thromboembolism

Out of all the seven patients with chronic pulmonary thromboembolism, we found total 26 thrombi. Out of which 1 (3.85%) thrombus was located at the central level, 11 (42.31%) thrombi were located at the segmental level, 12 (46.15%) thrombi were located at the subsegmental level, and two (7.69%) thrombi were located at the segmental level extending into subsegmental arteries

TABLE 11: Chronic pulmonary thromboembolism

Site of thrombus	No. of thrombus	Percentage
Central	1	3.85
Segmental	11	42.31
Subsegmental	12	46.15
Segmental +Subsegmental	2	7.69

**Fig. 17: Pie chart showing the proportion of various sites of thrombotic occlusion in patients with chronic pulmonary embolism scanned in dual-energy protocol****TABLE 12: Chronic Pulmonary thromboembolism**

Site of thrombus	No. of thrombus (after excluding one patient)	No. of perfusion defect	Perfusion defect %
Central	1	0	0.00
Segmental	9	2	22.2
Subsegmental	11	11	100
Segmental +Subsegmental	2	2	100
Total	231	15	65.22

In all the patients with chronic pulmonary thromboembolism, we correlated the finding with DEPI maps to determine whether that thrombus was causing perfusion defect on DEPI maps. Thrombus which cause perfusion defect on iodine maps are completely occluding thrombus, and thrombus which does not cause any perfusion defect on DEPI maps are either non-occluding or partially occluding thrombus.

Out of 7 patients with chronic pulmonary thromboembolism, we have excluded one patient from the evaluation of iodine perfusion maps due to significant associated lung parenchymal abnormality interfering with perfusion assessment .

After excluding one patient out of 7, the total thrombi seen were 23, and iodine perfusion defects were seen in 15 (65.22%) thrombi. The iodine perfusion defects were seen in zero out of one in central thrombi; two out of 9 (22.2%) in segmental thrombi; 11 out of 11 (100 %) in subsegmental thrombi; and two out of two (100 %) in segmental thrombi extending into subsegmental arteries

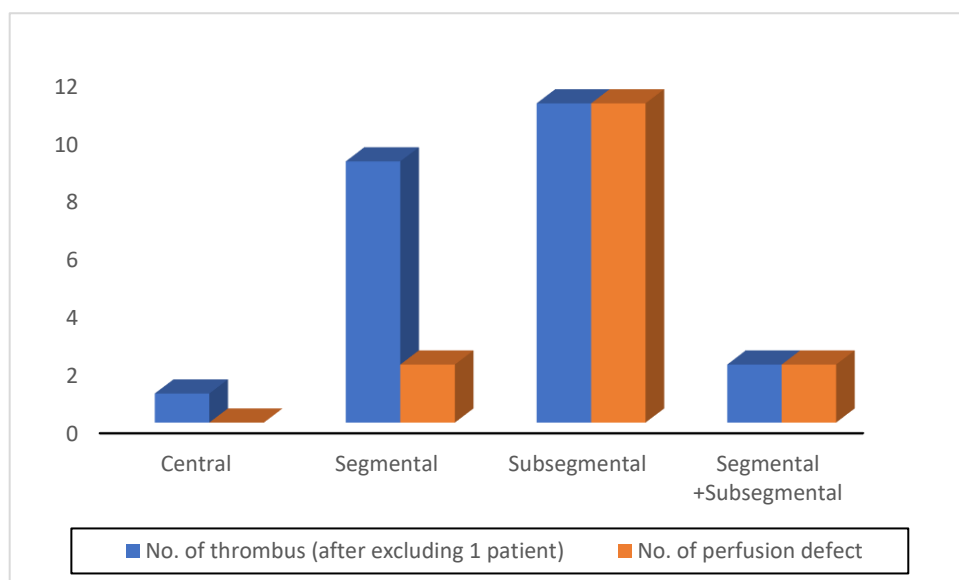


Fig. 18: Bar graph showing the proportion of patients with chronic pulmonary embolism with various sites of thrombotic occlusion showing perfusion defect on DEPI maps.

In three out of six patients with chronic pulmonary thromboembolism, it was difficult to see the thrombus by monoenergetic CTPA because it was eccentric and present at subsegmental level. However, the perfusion defects were seen on DEPI maps, and by retrospectively examining CTPA, thrombus were diagnosed confidently.

- In patients with acute pulmonary thromboembolism, we have calculated computed tomography obstructive index (CTOI) by examining the thrombus at all the levels (central, segmental, and subsegmental). CTOI was larger in a patient with central thrombus, which extends into segmental and subsegmental levels (maximum CTOI was 24). CTOI was less in patients with thrombus seen at a particular segment or only at segmental and subsegmental levels (minimum CTOI was 4).
- Out of all 13 patients with acute pulmonary embolism, a history of acute DVT was present in six (46.1 %) patients.

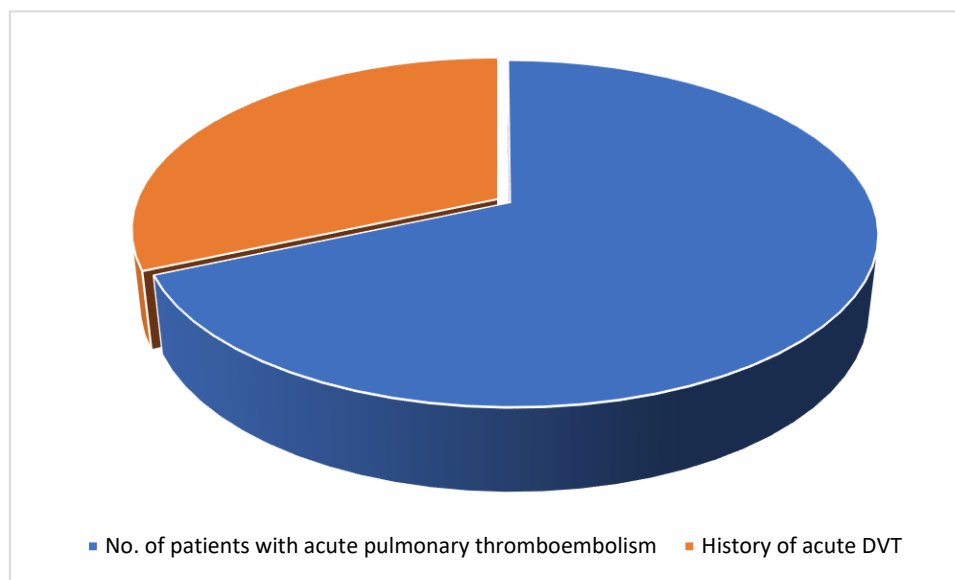


Fig. 19: Pie chart showing fraction of patients with acute pulmonary embolism having a history of acute DVT and scanned in dual-energy protocol

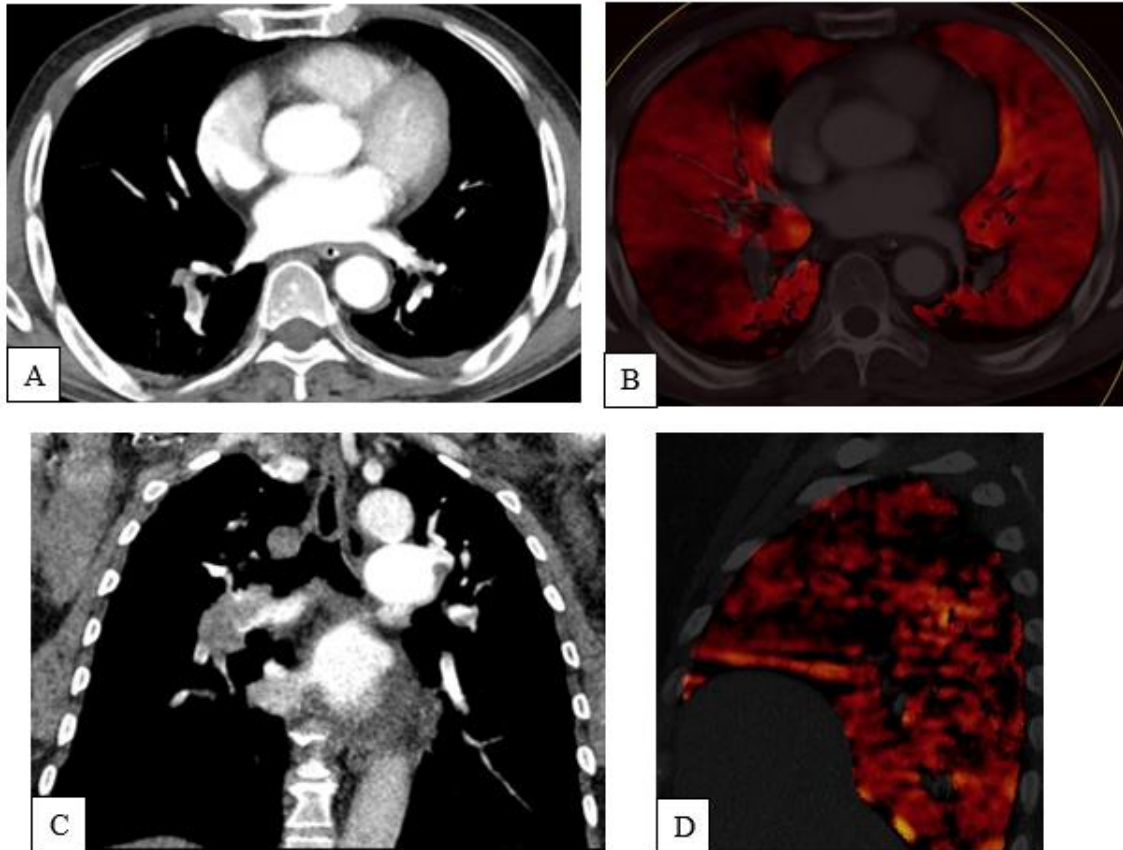


Fig. 21: Images showing acute pulmonary embolism at various levels and correlation with iodine maps

- A- Axial section of monoenergetic CTPA showing thrombus at segmental level
- B- Axial section of DEPI map of same patient (A) showing perfusion defect.
- C- Coronal section of monoenergetic CTPA showing thrombus in right pulmonary artery extending into segmental and subsegmental pulmonary arteries and
- D- Sagittal section of iodine perfusion map of right lung of same patient (C) showing perfusion defect in entire right lung on DEPI map

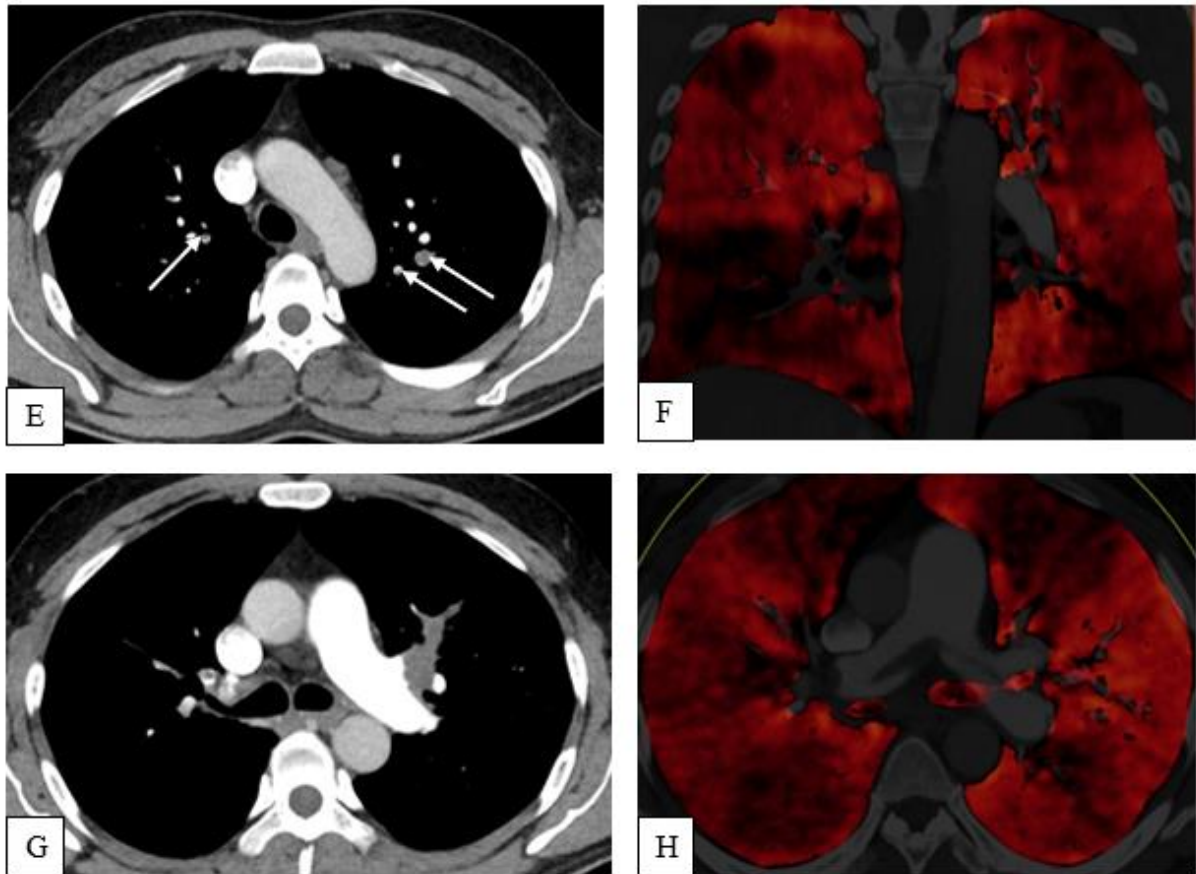


Fig. 21: Images showing acute pulmonary embolism at various levels and correlation with iodine maps.

E- Axial section of monoenergetic CTPA showing thrombus in subsegmental branches of apical segment of right upper lobe (arrow) and apicoposterior segment of left upper lobe (arrows).

F- Iodine map of same patient (E) showing defect in bilateral upper lobes corresponding to thrombi (defects in bilateral lower lobes are due to other thrombi).

G- Axial section of monoenergetic CTPA showing thrombus at segmental level extending into subsegmental branches of anterior segment of left upper lobe

H- Iodine map of same patient (G) showing characteristic wedge shape defect on iodine map in the anterior segment of left upper lobe. (Other filling defects in visualised bilateral lungs are due to other thrombi)

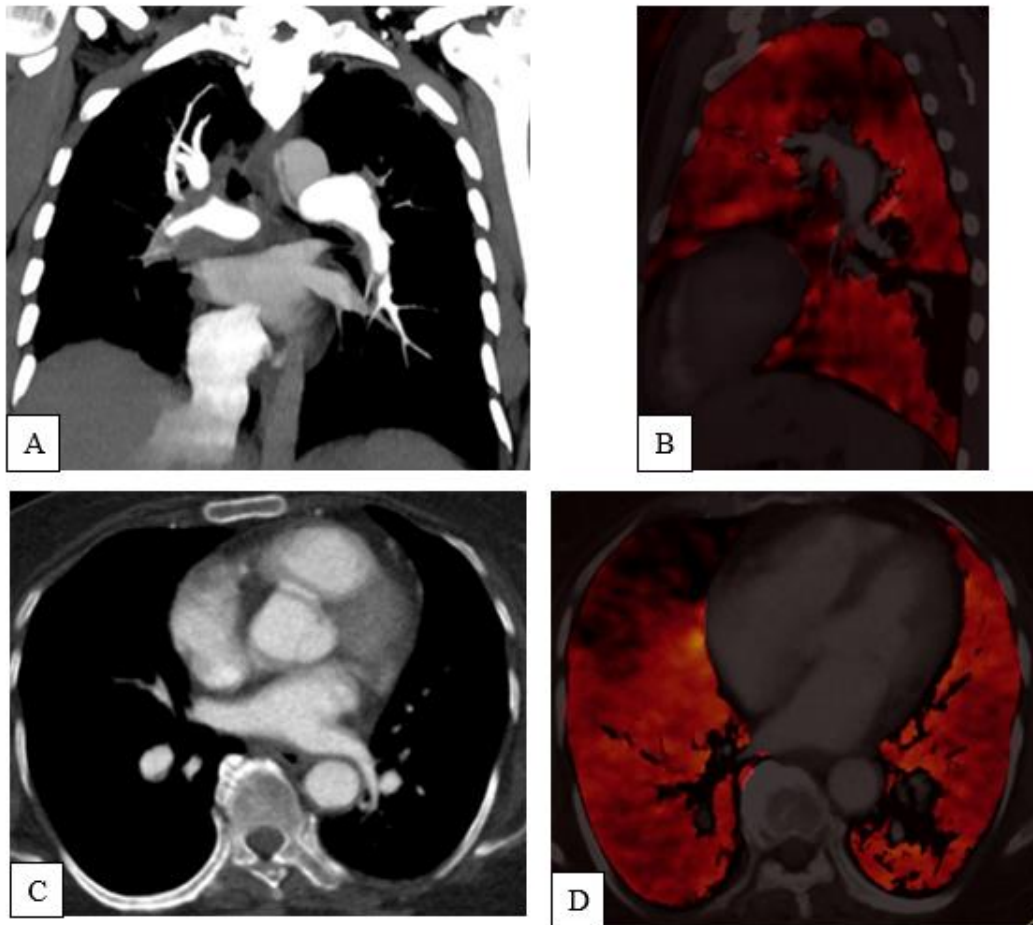


Fig 22: Images showing acute pulmonary embolism at various levels and correlation with iodine maps.

A-Coronal section of monoenergetic CTPA showing thrombus at segmental level (apicoposterior segment of left upper lobe).

B- Sagittal section of iodine map of left upper lobe of same patient (A) showing perfusion defect.

C- Axial section of monoenergetic CTPA showing thrombus at subsegmental level right middle lobe pulmonary arteries.

D- Axial section of iodine map of same patient (C) showing perfusion defect in right middle lobe on iodine map.

Discussion

PE has increasingly risen to the top of the list of urgent and severe illnesses seen in clinics because of recent advancements in imaging technologies and clinical diagnosis skills. PE is more likely to happen in older patients, those who have had a postoperative fracture, those who have spent a lot of time in bed, those who have malignant tumors, and those who have defective coagulation function.

The primary component of the thrombus is fibrin. Following its synthesis, the fibrinolytic system is activated, producing plasmin and lysing fibrin, whose disintegration releases certain degradation products such as D-dimers. (35) Although not extremely specific, the D-Dimer test is fairly sensitive (36,37). In addition to individuals with PE, other circumstances such as pregnancy, old age, infection, post-traumatic and post-operative setting, an inflammatory condition, and the presence of progressive neoplasia can also lead to a favorable outcome. In our study, the sensitivity of D-dimer in the prediction of pulmonary embolism is high (92 %), but specificity is low (16.13 %). Accordingly, the D-dimer assay's utility would be limited to excluding the diagnosis of PE when a normal result is linked to a low clinical probability of PE (38- 41).

DVT is a major risk factor for pulmonary embolism. According to a study by Lee Y H et al. (42), 68.2 % of patients with pulmonary embolism have DVT. In our study, out of 13 patients with acute pulmonary thromboembolism, six patients (46.1%) had a history of acute DVT.

Numerous studies show a connection between aging and an increased frequency of VTE (20,21). According to one study by Anderson FA Jr, Spencer FA patients over 40 years are much more at risk than younger patients, and the risk roughly doubles with each passing decade. In our study, it was also observed that patients older than 40 years developed

pulmonary thromboembolism, with the maximum number of patients falling in the age group of ≥ 60 years of age.

They concluded that the anatomical and pathological characteristics of PE are intimately related to both its clinical atypicality and fatality. Right heart failure results from an embolus in the pulmonary artery trunk and lobar arteries increasing the right ventricular load and pulmonary circulation pressure. Clinical signs are frequently more pronounced, and rapid death is frequently experienced. Because the region affected by the embolus is smaller and there is collateral circulation around the region, the clinical signs are typically not visible. The condition is frequently subacute or chronic when it affects the pulmonary segmental and subsegmental pulmonary arteries. However, the presence of an embolus in the peripheral pulmonary arteries slows blood flow, increases vorticity, lengthens mean transit time, and allows blood platelets to adhere to the pulmonary artery wall more readily (1).

The perfusion abnormalities brought on by PE may be better displayed by dual-source DECT perfusion imaging. Peripheral wedge-shaped perfusion defect is the most distinctive and specific perfusion defect to imply pulmonary embolism. When the embolus is present and does not totally occlude the vessel's lumen and allow the blood to pass through to prevent the major drop in perfusion, then the perfusion defect on the DEPI maps may not be present (1). The chances of getting a normal scan on DEPI maps (no filling defects on DEPI maps) are more in chronic pulmonary thromboembolism than acute pulmonary thromboembolism because, in chronic pulmonary thromboembolism, the thrombus is mostly eccentrically placed in pulmonary arteries and do not cause significant decrease in the perfusion in the parenchyma distal to the thrombus.

Perfusion images can also be masked by lung lesions such as pneumonia, pleural effusion, and pulmonary interstitial lesions. They might hamper DEPI figures. Finally, contrast chemicals in the heart cavity and veins, which can cause artifacts, may negatively affect the diagnostic

accuracy of DEPI pictures. DEPI is susceptible to a number of circumstances, yet it can detect variations in pulmonary perfusion. Therefore, a combined examination of CTPA and DEPI pictures is necessary to identify peripheral PE accurately (1).

Initial studies found that DECT had a higher radiation exposure than single-energy CT in terms of radiation dosage (4,22). According to some previous studies, DECT does not require additional radiation dose compared to a single energy scan (23,24). According to our study, the radiation exposure in DECT is more than monoenergetic CTPA, with a mean radiation dose of 1.59 mSV and 1.06 mSV for DECT and monoenergetic CTPA, respectively. To minimize the increase in radiation exposure, dose-reduction strategies, including selective photon shield usage and tube current control, would be helpful (25,26).

Third-generation DECT's advancements in dual-energy voltage combination, larger thin filters, and more exact spectral separation of X-rays enable CTPA examinations with lower radiation exposure while maintaining image quality than those using second-generation DECT or single-energy CT (27-29).

According to one study by Lenga et al. the mean effective radiation dose on third generation CT scanner for single energy CTPA was (1.5 mSv \pm 0.8 mSv) and for DECT was (1.4 mSv \pm 0.7 mSv). The effective radiation dose on third generation dual source CT was significantly lower than second generation dual source CT. (37)

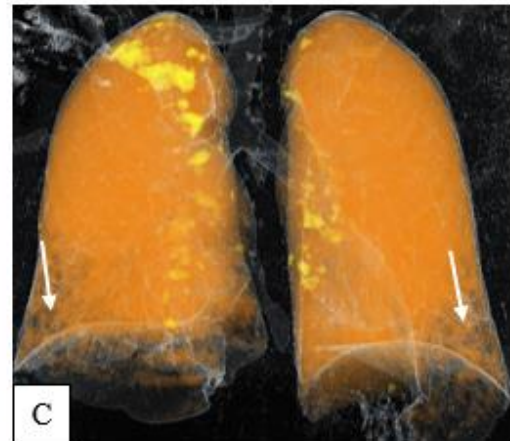
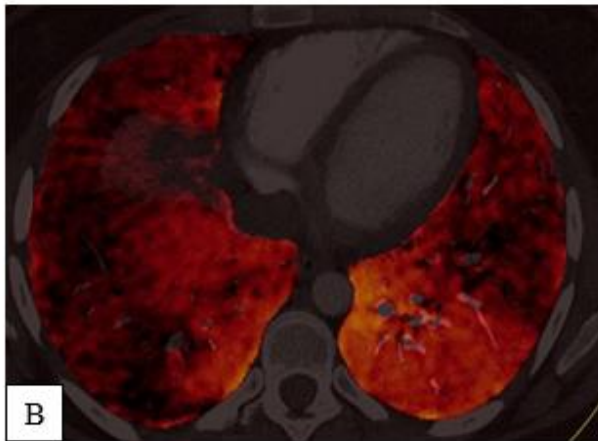
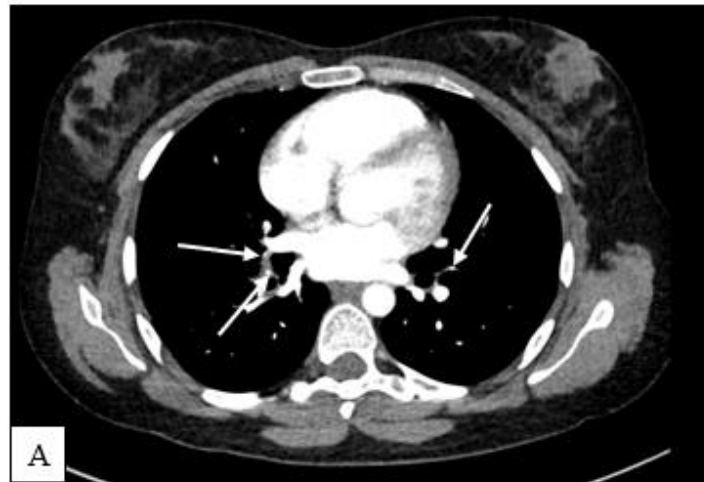
In our study, acute thrombi were seen at central level were 11 (8.4%), at segmental level were 39 (29.77%), at subsegmental level were 14 (10.69%), at segmental level extending into subsegmental pulmonary arteries were 66 patients (29.77%) and at central level extending into segmental and subsegmental pulmonary arteries was one (0.76%). For chronic thromboembolism, thrombi seen at central level was 1 (3.85%), at segmental level were 11 (42.31%), at subsegmental level were 12 (10.69%), at segmental level extending into subsegmental pulmonary arteries were two patients (7.69%). Thrombi seen at the central level

are very less, and maximum thrombi are seen at segmental and subsegmental levels, which is consistent with the study conducted by Okada M et al. (17)

CTOI is larger in patients with central thrombus, which extends into segmental and subsegmental levels, and in patients in which thrombus is seen at a particular segment or only at segmental and subsegmental levels. This is in line with the findings of the study by Okada M et al. (17), which found that individuals with central intrapulmonary clots had greater CTOI. With the proliferation of MDCT scanners, recent developments in CT technology have made it possible to scan larger volumes more quickly and with thinner collimation, improving the visualization of segmental and subsegmental pulmonary arteries and interobserver agreement regarding the presence or absence of pulmonary embolism (30).

Small peripheral embolisms may still go undetected despite radiologists having to review over 300 axial images to do so (31-33). In our study also, some peripheral intrapulmonary thrombi were also missed, even when thin-slice CTPA images were used. According to our study, chronic thromboembolism has a higher risk of peripheral thrombi being missed (at the subsegmental level) than acute pulmonary thromboembolism. This is due to the thrombus' eccentric presence in the pulmonary arteries, which the observer may miss in chronic thromboembolism. Low kilovoltage CT scanning is used for CTPA to increase the percentage of central and peripheral pulmonary arteries that can be evaluated with CTPA without a significant reduction in image quality. This is because the enhancement by iodinated contrast material increases as the effective energy of the X-ray beam decreases and comes closer to the maximum absorption close to the k-edge of iodine (34).

CASE 1



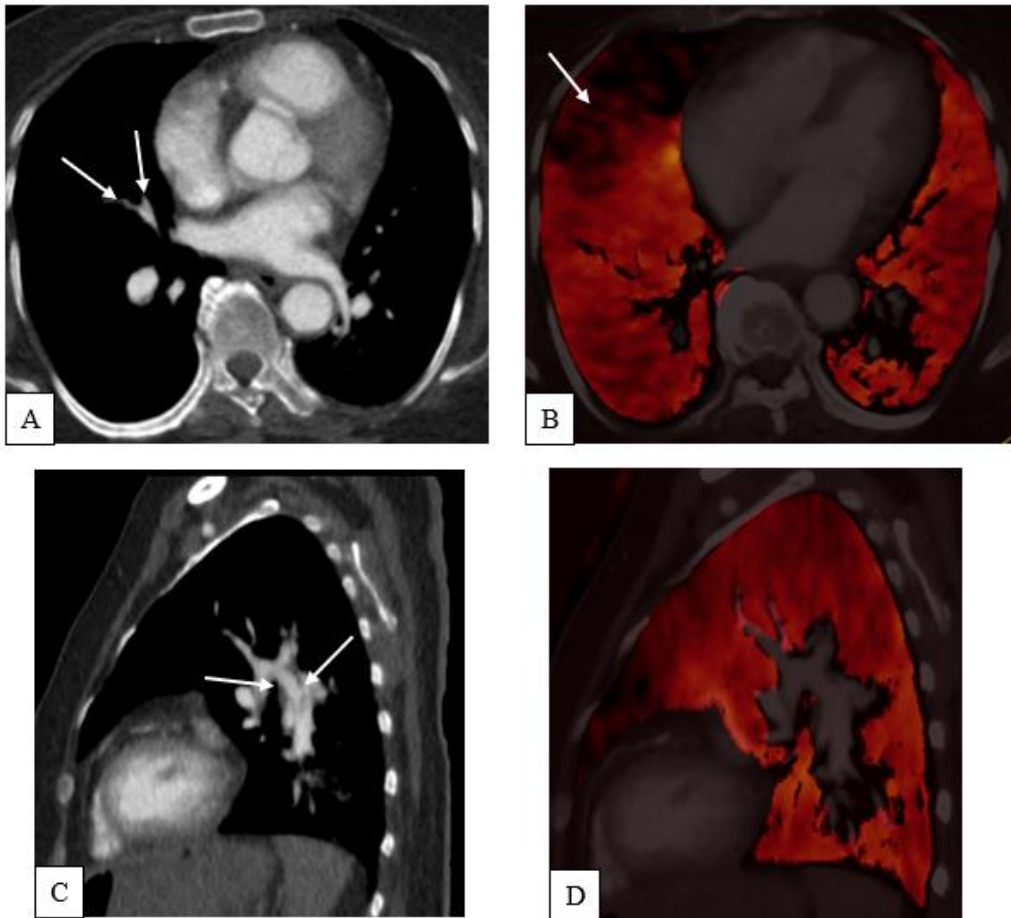
23-year-old lady presents with fever and SOB for 15 days. On workup diagnosed to have “Warm Antibody Haemolytic Anemia”.

A- CTPA imaging shows eccentric thrombi (arrows) with luminal narrowing in bilateral lower lobes.

B- DEPI map showing perfusion defects in the bilateral lower lobes corresponding to the filling defects in figure A. Subtle findings in CTPA are reflected as large perfusion defects on DEPI map.

C- VRT image of dual energy CTPA showing filling defects (arrows) in bilateral lower lobes.

CASE 2



Follow up patient of pulmonary embolism.

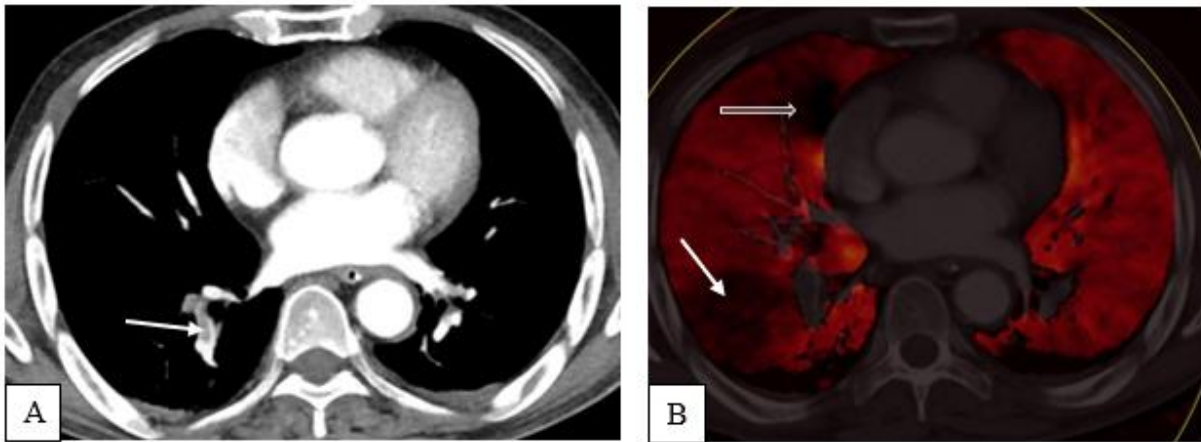
A- CTPA imaging shows small thrombi (blue arrows) in right middle lobe segmental arteries causing complete luminal obstruction.

B-DEPI map showing large perfusion defect in the right middle lobe.

Thrombus in figure A is small, that could be missed on normal CTPA but causing large perfusion defect on DEPI map.

C and D - shows multiple non occluding thrombi not causing any perfusion defect on DEPI map.

CASE 3



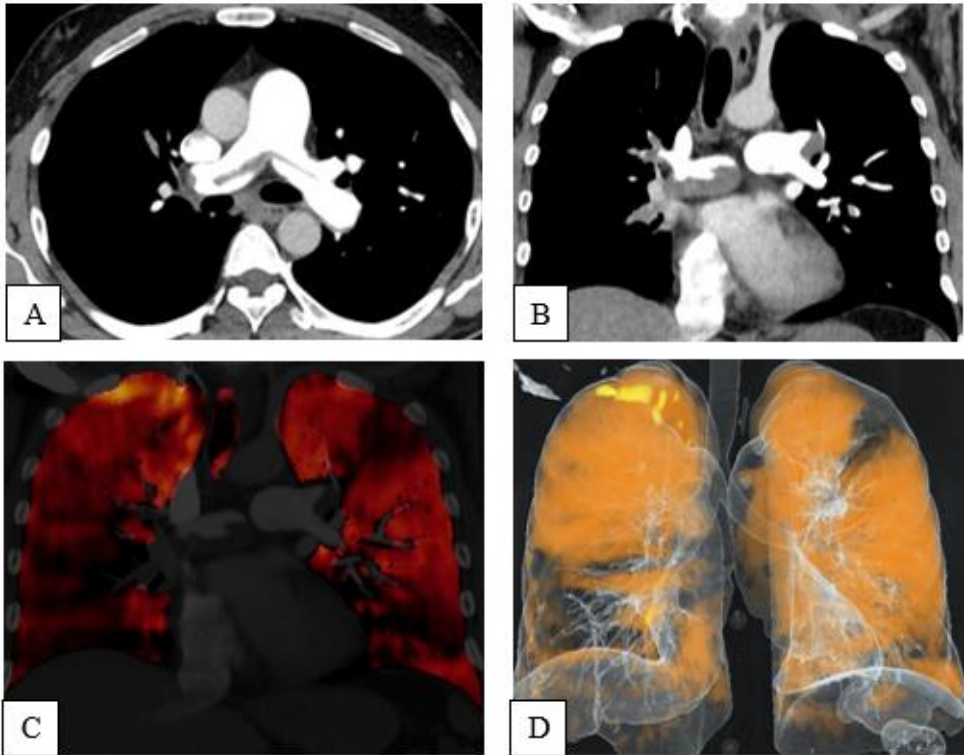
Post-operative case of bowel obstruction. C/O right chest pain and breathlessness.

A- CTPA imaging shows small thrombi in the basal segments of right lower lobe, but causing complete luminal occlusion of lateral basal segmental artery (white solid arrow).

B- DEPI map showing large wedge-shaped perfusion defect in the lateral basal segment of right lower lobe (white solid arrow).

Right middle lobe medial segment perfusion deficit is caused by artefact from heart pulse (white block arrow).

CASE 4



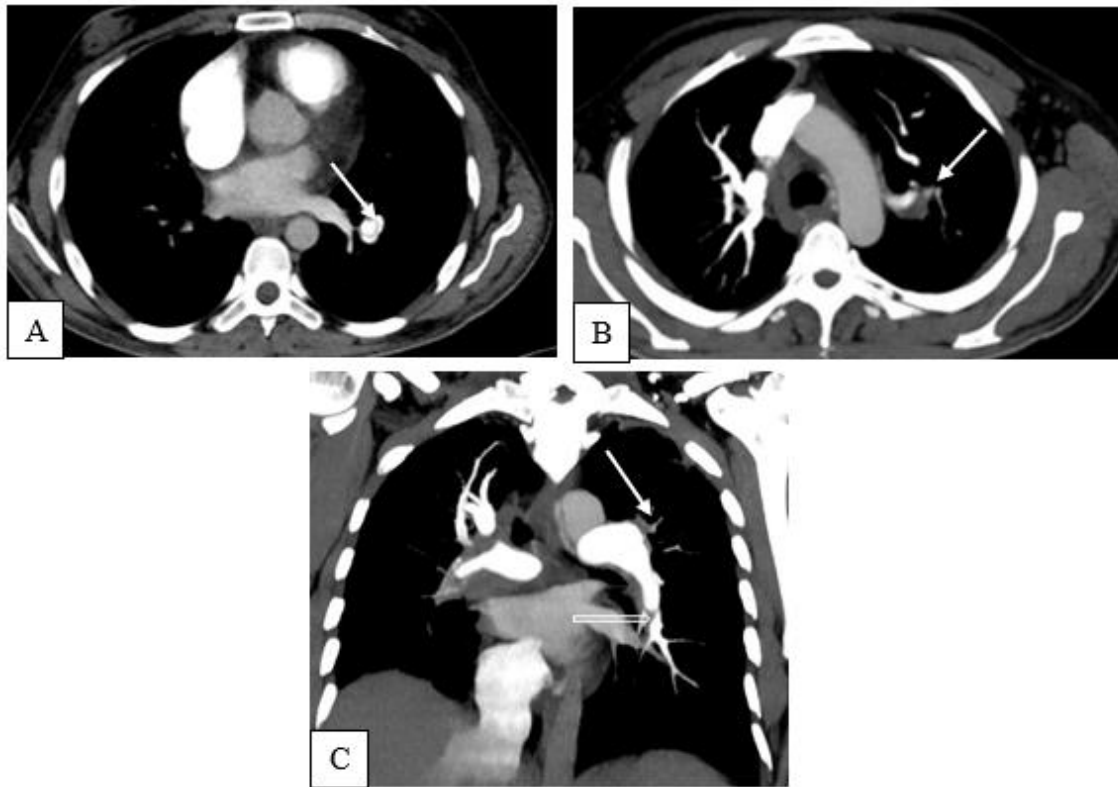
Patient has left lower limb pain and swelling and breathlessness. On USG- DVT of left lower limb.

A- CTPA imaging showing “Saddle thrombus”. Saddle thrombus means thrombus present at bifurcation of pulmonary trunk and extending into left and right pulmonary arteries.

B- CTPA imaging shows filling defects in segmental and subsegmental vessels of bilateral lungs.

C- DEPI map shows perfusion defects in the bilateral lungs with characteristic wedge-shaped perfusion defects in left upper and lower lobe.

CASE 5



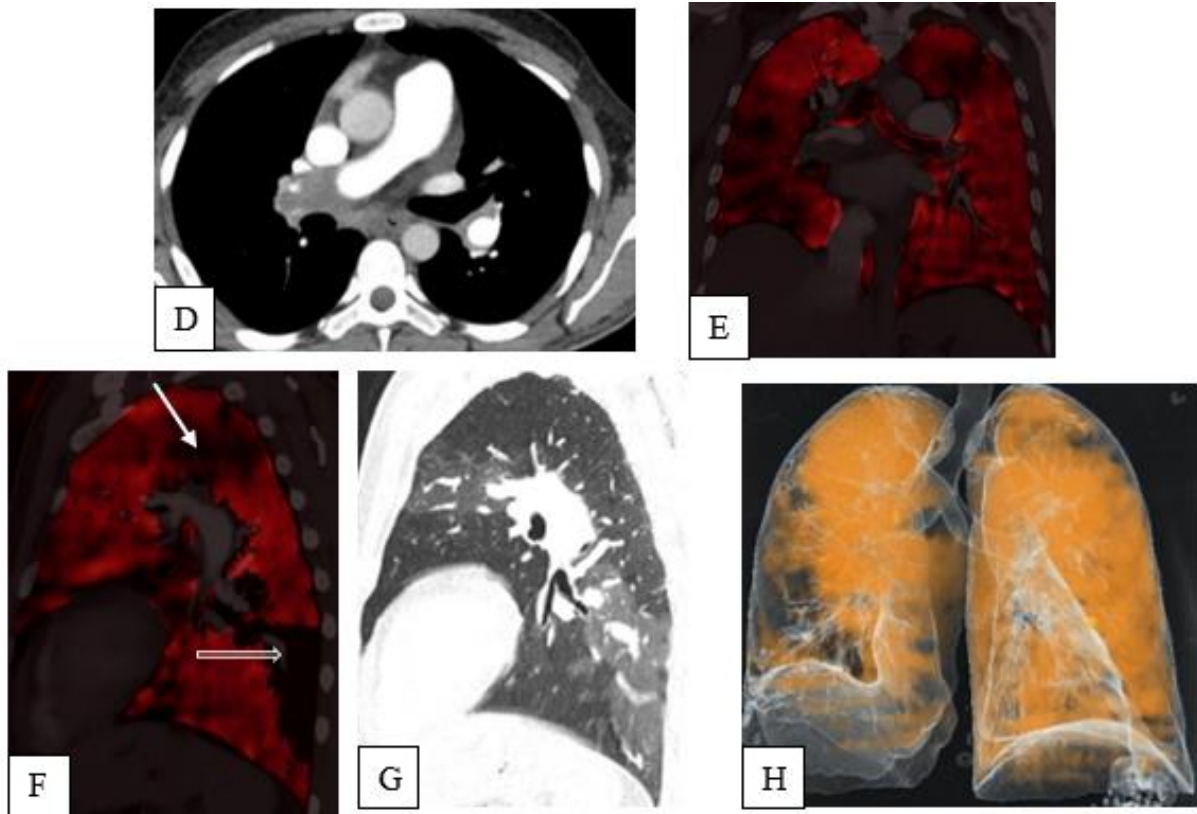
Patient has history of left lower limb DVT (stopped warfarin 2 months back), now patient is having gradually progressive breathlessness.

A- CTPA imaging showing “web” like thrombus (arrow) in left lower lobe pulmonary artery- suggestive of chronic thromboembolism.

B- CTPA, MIP image showing eccentric filling defect (arrow) in apico-posterior segmental branch of left pulmonary artery causing complete luminal occlusion.

C- CTPA, MIP image showing

- Filling defect (white solid arrow) in apico-posterior segmental branch of left pulmonary artery causing complete luminal occlusion.
- “Webb” like filling thrombus (white block arrow) in left lower lobe pulmonary artery.



D- CTPA imaging showing complete luminal occlusion of right pulmonary artery with sparing of right upper lobe branches (shown in Fig. B)- suggestive of acute thrombus.

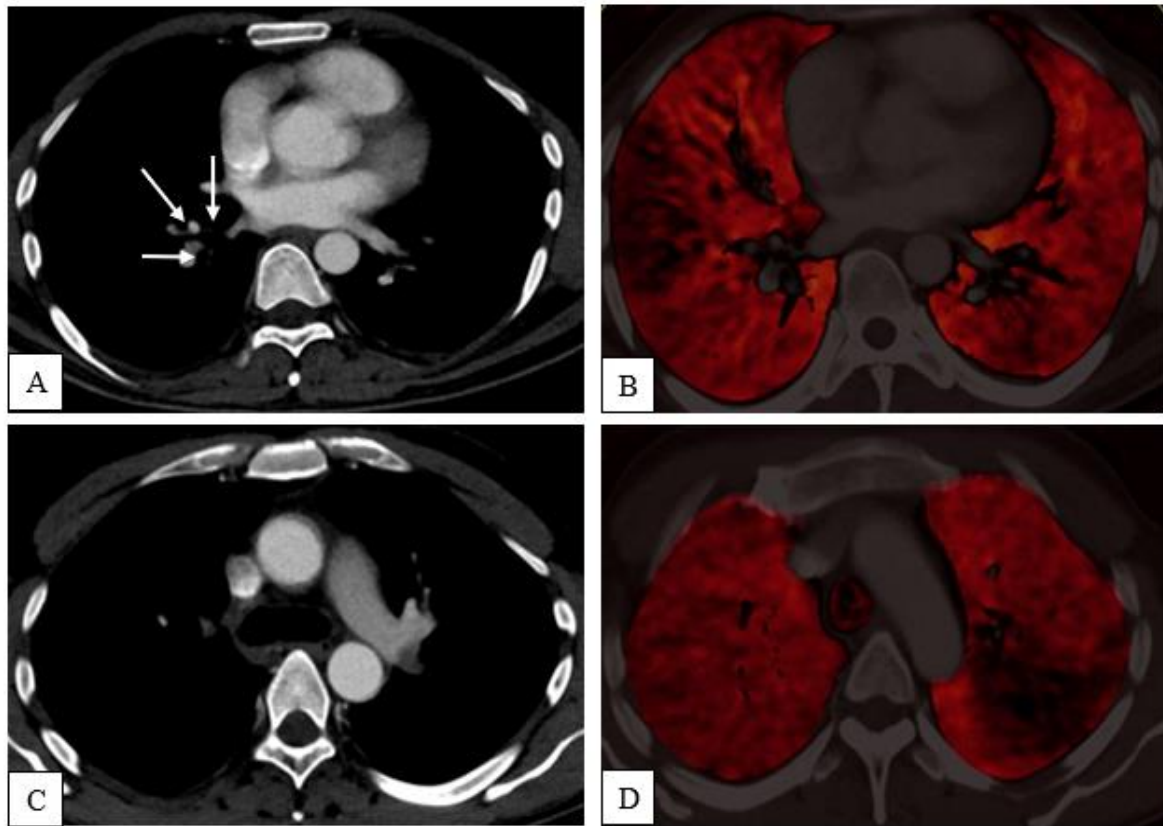
E- DEPI map showing large perfusion defects in right middle and lower lobe and apicoposterior segment of left upper lobe.

F- DEPI map showing perfusion defect in apicoposterior segment of left upper lobe (white solid arrow). Perfusion defect in superior and posterior basal segments of left lower lobe (white block arrow) are due to abnormal parenchyma (shown in coronal section of lung window in Fig. G).

H- VRT image showing filling defects in right middle lobe, right lower lobe and apicoposterior segment of left upper lobe.

So the patient has acute on chronic thromboembolism.

CASE 6



Patient having history of sudden onset breathlessness with drop in the oxygen saturation levels.

A- CTPA imaging showing thrombus in the segmental branches of right lower lobe arteries(arrows) but causing complete luminal obstruction of right lateral basal segmental artery.

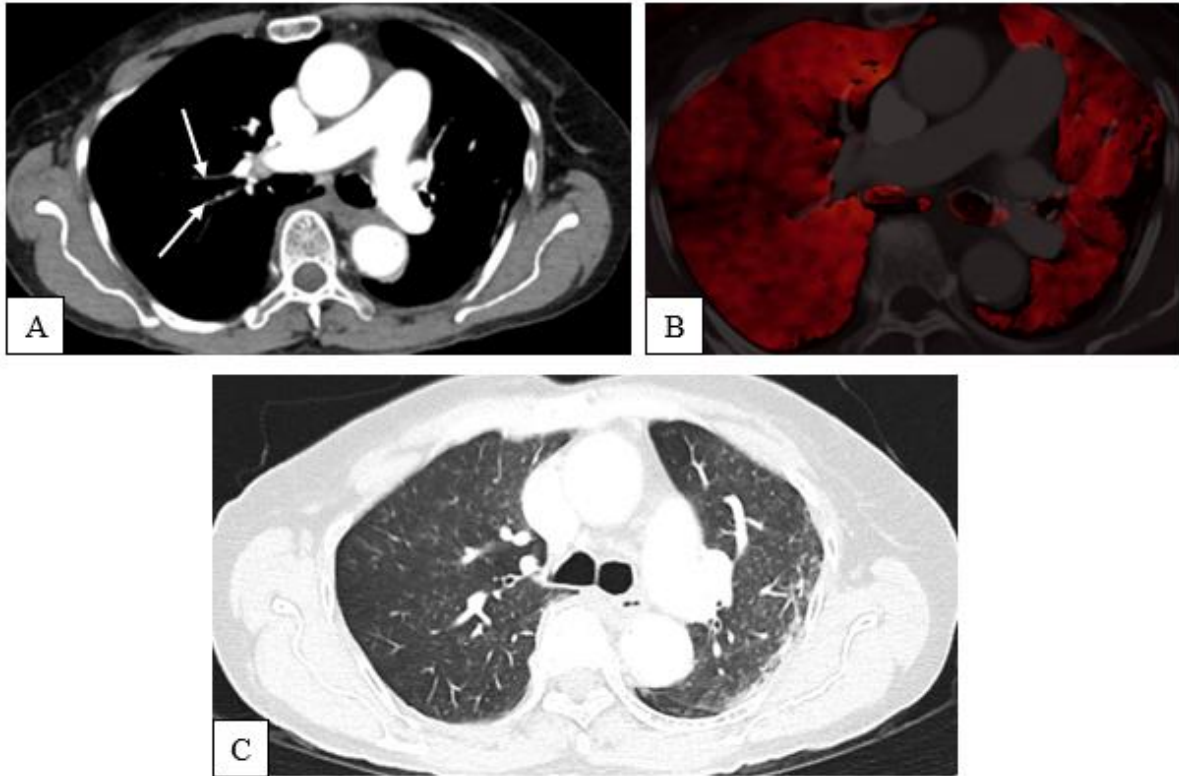
B- DEPI map shows wedge shaped perfusion defects in the lateral basal segment of right lower lobe because of complete luminal obstruction of segmental artery (shown in FIG. A).

Complete luminal obstruction of segmental artery in apicoposterior segment of left upper lobe (Fig. C- blue arrow) reflected as wedge shaped perfusion defect (Fig. D and F)



Multiple filling defect in basal segmental branches of left pulmonary artery not causing significant luminal obstruction (Fig. E) and not showing any perfusion defect on left lower lobe (Fig. F).

CASE 7

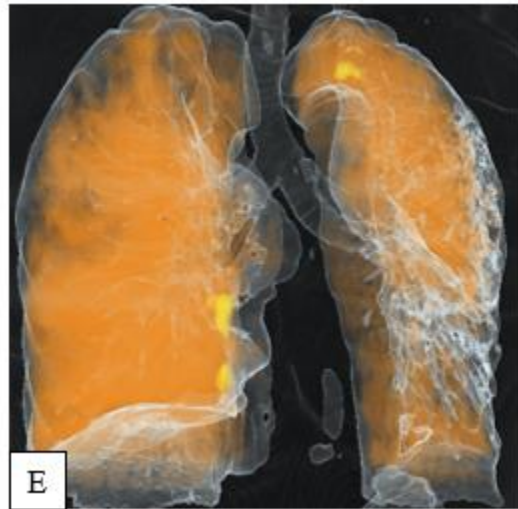
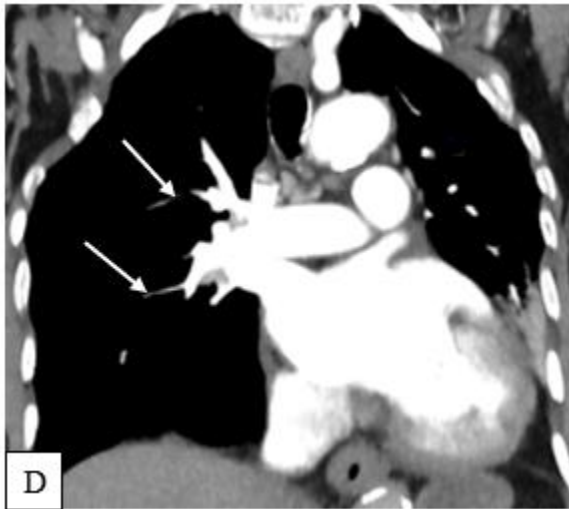


Past history of fracture femur. Now presented with complaint of difficulty in breathing and drop in the saturation.

A- CTPA imaging showing pruning of pulmonary vessels (arrows) in right upper lobe.

B- DEPI map shows perfusion defects in right upper lobe. Perfusion defects in left upper lobe is due to abnormal pulmonary parenchyma (shown in axial section of HRCT chest in Fig. C).

These subtle findings were missed on CTPA but created large filling defects on DEPI map. Retrospectively able to detect these subtle findings.



D- CTPA imaging showing pruning of pulmonary vessels (arrows) in right upper lobe.

E- VRT image of dual-energy pulmonary angiography showing filling defects in right upper lobe and right middle lobe. Filling defects in left lung is due to abnormal parenchyma.

Conclusion

- DEPI maps along with CTPA can detect more acute as well as chronic pulmonary thromboembolism, specifically at the small segmental and subsegmental pulmonary arterial levels.
- A pulmonary thromboembolism that is partially occluding or non-occluding does not decrease the lung perfusion and may not be clinically symptomatic compared with occluding thrombus causing perfusion defect. So, by using the DEPI maps, we can differentiate occluding and non-occluding thrombus, which helps in clinical management.
- Although, in our study the effective radiation dose of third generation DECT is higher than in single source CTPA. However, the radiation dose is significantly lower than the dose in second generation DECT as published in previous literatures.
- Iodine perfusion defects can be seen due to parenchymal abnormality or other artifacts. Hence, combined assessment using CTPA and DEPI maps increases the diagnostic accuracy of detection of pulmonary embolism.
- D-dimer has high sensitivity but low specificity for the detection of pulmonary embolism.

Limitations of our study

- The main limitation of our study was the small sample size (73 patients), which was impacted due to time constraints.
- It was a nonrandomized study. Randomization will allow better comparison of DECT versus single energy CTPA.
- It was a single-center study. A multicentric study across different parts of the country with a larger sample size is needed to generalize the result to the population.

BIBLIOGRAPHY

1. Mao X, Wang S, Jiang X, Zhang L, Xu W. Diagnostic value of dual-source computerized tomography combined with perfusion imaging for peripheral pulmonary embolism. *Iran J Radiol.* 2016 Apr;13(2) :e29402.
2. Zhang J, Cai J, Liu S, Zhang X. Value of dual-energy lung perfusion imaging using a dual-source CT system for the pulmonary embolism. *Open Life Sci.* 2018 Jan 1;13(1):107-11.
3. Palm V, Rengier F, Rajiah P, Heussel CP, Partovi S. Acute pulmonary embolism: imaging techniques, findings, endovascular treatment and differential diagnoses. *Rofo.* 2020 Jan;192(1):38-49.
4. Hong YJ, Shim J, Lee SM, Im DJ, Hur J. Dual-energy CT for pulmonary embolism: current and evolving clinical applications. *Korean J Radiol.* 2021 Sep;22(9):1555-68.
5. Thieme SF, Meinel FG, Graef A, Helck AD, Reiser MF, Johnson TR. Dual-energy CT pulmonary angiography in patients with suspected pulmonary embolism: value for the detection and quantification of pulmonary venous congestion. *Br J Radiol.* 2014 Jul;87(1039):20140079.
6. Ghaye B. Peripheral pulmonary embolism on multidetector CT pulmonary angiography. *JBR-BTR.* 2007 Mar 1;90(2):100-8.
7. Grob D, Smit E, Prince J, Kist J, Stöger L, Geurts B, et al. Iodine maps from subtraction CT or dual-energy CT to detect pulmonary emboli with CT angiography: a multiple-observer study. *Radiology.* 2019 Jul;292(1):197-205.
8. Giordano NJ, Jansson PS, Young MN, Hagan KA, Kabrhel C. Epidemiology, pathophysiology, stratification, and natural history of pulmonary embolism. *Tech Vasc Interv Radiol.* 2017 Sep 1;20(3):135-40.

9. Shen W, Liu H, Zhu P, Chen Y, Qiao H, Su G, et al. Diagnostic Value of the Dual Source CT Dual Energy Pulmonary Perfusion Imaging for Pulmonary Embolism. *Zhongguo Yi Xue Ke Xue Yuan Xue Bao*. 2020 Oct;42(5):646-650.
10. Weidman EK, Plodkowski AJ, Halpenny DF, Hayes SA, Perez-Johnston R, Zheng J, et al. Dual-energy CT angiography for detection of pulmonary emboli: incremental benefit of iodine maps. *Radiology*. 2018 Nov;289(2):546-53.
11. Im DJ, Hur J, Han K, Suh YJ, Hong YJ, Lee HJ, et al. Prognostic Value of Dual-Energy CT-Based Iodine Quantification versus Conventional CT in Acute Pulmonary Embolism: A Propensity-Match Analysis. *Korean J Radiol*. 2020 Sep;21(9):1095-1103.
12. Grob D, Smit E, Oostveen LJ, Snoeren MM, Prokop M, Schaefer-Prokop CM, et al. Image quality of iodine maps for pulmonary embolism: a comparison of subtraction CT and dual-energy CT. *AJR Am J Roentgenol*. 2019 Jun;212(6):1253-9.
13. Thieme SF, Johnson TR, Lee C, McWilliams J, Becker CR, Reiser MF, et al. Dual-energy CT for the assessment of contrast material distribution in the pulmonary parenchyma. *AJR Am J Roentgenol*. 2009 Jul;193(1):144-9.
14. Bauer RW, Frellesen C, Renker M, Schell B, Lehnert T, Ackermann H, et al. Dual energy CT pulmonary blood volume assessment in acute pulmonary embolism - correlation with D-dimer level, right heart strain and clinical outcome. *Eur Radiol*. 2011 Sep;21(9):1914-21.
15. Fink C, Johnson TR, Michaely HJ, Morhard D, Becker C, Reiser M, et al. Dual-energy CT angiography of the lung in patients with suspected pulmonary embolism: initial results. *Rof*. 2008 Oct;180(10):879-83.
16. Hansmann J, Fink C, Jost G, Pietsch H, Meyer M, Nance JW Jr, et al. Impact of iodine delivery rate with varying flow rates on image quality in dual-energy CT of patients with suspected pulmonary embolism. *Acad Radiol*. 2013 Aug;20(8):962-71.

17. Okada M, Kunihiro Y, Nakashima Y, Nomura T, Kudomi S, Yonezawa T, et al. Added value of lung perfused blood volume images using dual-energy CT for assessment of acute pulmonary embolism. *Eur J Radiol.* 2015 Jan;84(1):172-177.
18. McCollough CH, Leng S, Yu L, Fletcher JG. Dual-and multi-energy CT: principles, technical approaches, and clinical applications. *Radiology.* 2015 Sep;276(3):637-53.
19. Wittram C, Kalra MK, Maher MM, Greenfield A, McLoud TC, Shepard JA. Acute and chronic pulmonary emboli: angiography–CT correlation. *AJR Am J Roentgenol.* 2006 Jun;186(6 Suppl 2):S421-9.
20. Muscedere JG, Heyland DK, Cook D. Venous thromboembolism in critical illness in a community intensive care unit. *J Crit Care.* 2007 Dec;22(4):285-9.
21. Torbicki A, Perrier A, Konstantinides S, Agnelli G, Galiè N, Pruszczyk P, et al. ESC Committee for Practice Guidelines (CPG). Guidelines on the diagnosis and management of acute pulmonary embolism: the Task Force for the Diagnosis and Management of Acute Pulmonary Embolism of the European Society of Cardiology (ESC). *Eur Heart J.* 2008 Sep;29(18):2276-315.
22. Stein PD, Sostman HD, Bounameaux H, Buller HR, Chenevert TL, Dalen JE, et al. Challenges in the diagnosis of acute pulmonary embolism. *Am J Med.* 2008 Jul;121(7):565-71.
23. Fedullo PF, Tapson VF. Clinical practice. The evaluation of suspected pulmonary embolism. *N Engl J Med.* 2003 Sep 25;349(13):1247-56.
24. Stein PD, Hull RD, Patel KC, Olson RE, Ghali WA, Brant R, et al. D-dimer for the exclusion of acute venous thrombosis and pulmonary embolism: a systematic review. *Ann Intern Med.* 2004 Apr 20;140(8):589-602.

25. Wells PS, Anderson DR, Rodger M, Stiell I, Dreyer JF, Barnes D, et al. Excluding pulmonary embolism at the bedside without diagnostic imaging: management of patients with suspected pulmonary embolism presenting to the emergency department by using a simple clinical model and d-dimer. *Ann Intern Med.* 2001 Jul 17;135(2):98-107.
26. Perrier A, Desmarais S, Miron MJ, de Moerloose P, Lepage R, Slosman D, et al. Non-invasive diagnosis of venous thromboembolism in outpatients. *Lancet.* 1999 Jan 16;353(9148):190-5
27. Lee YH, Cha SI, Shin KM, Lim JK, Lee WK, Park JE, et al. Clinical characteristics and outcomes of patients with isolated pulmonary embolism. *Blood Coagul Fibrinolysis.* 2021 Sep 1;32(6):387-393.
28. Nicolaides AN, Fareed J, Kakkar AK, Comerota AJ, Goldhaber SZ, Hull R, et al. Prevention and treatment of venous thromboembolism--International Consensus Statement. *Int Angiol.* 2013 Apr;32(2):111-260.
29. Anderson FA Jr, Spencer FA. Risk factors for venous thromboembolism. *Circulation.* 2003 Jun 17;107(23 Suppl 1):I9-16.
30. Henzler T, Fink C, Schoenberg SO, Schoepf UJ. Dual-energy CT: radiation dose aspects. *AJR Am J Roentgenol.* 2012 Nov;199(5 Suppl): S16-25.
31. Johnson TR, Krauss B, Sedlmair M, Grasruck M, Bruder H, Morhard D, et al. Material differentiation by dual energy CT: initial experience. *Eur Radiol.* 2007 Jun;17(6):1510-7.
32. Schenzle JC, Sommer WH, Neumaier K, Michalski G, Lechel U, Nikolaou K et al. Dual energy CT of the chest: how about the dose? *Invest Radiol.* 2010 Jun;45(6):347-53.

33. Hong YJ, Kim JY, Choe KO, Hur J, Lee HJ, Choi BW, et al. Different perfusion pattern between acute and chronic pulmonary thromboembolism: evaluation with two-phase dual-energy perfusion CT. *AJR Am J Roentgenol.* 2013 Apr;200(4):812-7.
34. Matsubara K, Takata T, Kobayashi M, Kobayashi S, Koshida K, Gabata T. Tube Current Modulation Between Single- and Dual-Energy CT With a Second-Generation Dual-Source Scanner: Radiation Dose and Image Quality. *AJR Am J Roentgenol.* 2016 Aug;207(2):354-61
35. Krauss B, Grant KL, Schmidt BT, Flohr TG. The importance of spectral separation: an assessment of dual-energy spectral separation for quantitative ability and dose efficiency. *Invest Radiol.* 2015 Feb;50(2):114-8.
36. Lenga L, Leithner D, Peterke JL, Albrecht MH, Gudauskas T, D'Angelo T, et al. Comparison of Radiation Dose and Image Quality of Contrast-Enhanced Dual-Source CT of the Chest: Single-Versus Dual-Energy and Second-Versus Third-Generation Technology. *AJR Am J Roentgenol.* 2019 Apr;212(4):741-7.
37. Lenga L, Trapp F, Albrecht MH, Wichmann JL, Johnson AA, Yel I, et al. Single- and dual-energy CT pulmonary angiography using second- and third-generation dual-source CT systems: comparison of radiation dose and image quality. *Eur Radiol.* 2019 Sep;29(9):4603-12.
38. Patel S, Kazerooni EA, Cascade PN. Pulmonary embolism: optimization of small pulmonary artery visualization at multi-detector row CT. *Radiology.* 2003 May;227(2):455-60.
39. Le Gal G, Righini M, Parent F, van Strijen M, Couturaud F. Diagnosis and management of subsegmental pulmonary embolism. *J Thromb Haemost.* 2006 Apr;4(4):724-31.

40. Ghanima W, Nielszen BE, Holmen LO, Witwit A, Al-Ashtari A, Sandset PM. Multidetector computed tomography (MDCT) in the diagnosis of pulmonary embolism: interobserver agreement among radiologists with varied levels of experience. *Acta Radiol.* 2007 Mar;48(2):165-70
41. Brunot S, Corneloup O, Latrabe V, Montaudon M, Laurent F. Reproducibility of multi-detector spiral computed tomography in detection of sub-segmental acute pulmonary embolism. *Eur Radiol.* 2005 Oct;15(10):2057-63.
42. Sigal-Cinqualbre AB, Hennequin R, Abada HT, Chen X, Paul JF. Low-kilovoltage multi-detector row chest CT in adults: feasibility and effect on image quality and iodine dose. *Radiology.* 2004 Apr;231(1):169-74.

Patient information sheet

1. Risks to the patients: There's no risk of death or any disability resulting directly due to imaging. No interventions or life-threatening procedures will be done.
2. Confidentiality: Your participation will be kept confidential. Your medical records will be treated with confidentiality and will be revealed only to doctors/ scientists involved in this study. The results of this study may be published in a scientific journal, but you will not be identified by name.
3. Provision of free treatment for research related injury: Not applicable.
4. Compensation of subjects for disability or death resulting from such injury: Not applicable.
5. You have complete freedom to participate and to withdraw from research at any time without penalty or loss of benefits to which you would otherwise be entitled, including subsequent medical treatment or relationship with the treating physician.
6. Your participation in the study is optional and voluntary.
7. The copy of the results of the investigations performed will be provided to you for your record.

रोगी सूचना पत्रक

1. मरीजों के लिए जोखिम: इमेजिंग के कारण मौत या किसी भी विकलांगता का कोई खतरा नहीं है। कोई हस्तक्षेप या जानलेवा प्रक्रिया नहीं की जाएगी।
2. गोपनीयता: आपकी भागीदारी गोपनीय रखी जाएगी। आपके मेडिकल रिकॉर्ड का उपयोग गोपनीयता के साथ किया जाएगा और इस अध्ययन में शामिल डॉक्टरों / वैज्ञानिकों के लिए ही खुलासा किया जाएगा। इस अध्ययन के परिणाम वैज्ञानिक पत्रिका में प्रकाशित किए जा सकते हैं, लेकिन आपको नाम से पहचाना नहीं जाएगा।
3. अनुसंधान से संबंधित चोट के लिए निः शुल्क उपचार की व्यवस्था: लागू नहीं है।
4. ऐसी चोट से होने वाली विकलांगता या मृत्यु के लिए मुआवजा: लागू नहीं है।
5. आपके पास किसी भी समय जुर्माना या नुकसान के बिना अनुसंधान से वापसी की पूर्ण स्वतंत्रता है।
6. अध्ययन में आपकी भागीदारी वैकल्पिक और स्वैच्छिक है।
7. किए गए जांच के परिणामों की रिकॉर्ड आपको प्रदान की जाएगी।

All India Institute of Medical Sciences Jodhpur, Rajasthan
Informed Consent Form

Title of the project: **Role of Dual-Energy Computed Tomography (DECT) in Pulmonary Embolism.**

Name of the Principal Investigator : Dr. Satish Kumar (8057617636)

Patient/Volunteer Identification No. :

I, _____ S/o or D/o _____
R/o _____

give my full, free, voluntary consent to be a part of the study “Role of Dual-Energy Computed Tomography (DECT) in Pulmonary Embolism” the procedure and nature of which has been explained to me in my own language to my full satisfaction. I confirm that I have had the opportunity to ask questions.

I understand that my participation is voluntary, and I am aware of my right to opt out of the study at any time without giving any reason.

I understand that the information collected about me and any of my medical records may be looked at by responsible individual from _____(Company Name) or from regulatory authorities. I give permission for these individuals to have access to my records.

Date : _____

Place : _____ Signature/Left thumb impression

This to certify that the above consent has been obtained in my presence.

Date : _____

Place : _____ Signature of Principal Investigator

Witness 1

Signature

Name: _____

Address : _____

Witness 2

Signature

Name: _____

Address : _____

अखिल भारतीय आयुर्विज्ञान संस्थान जोधपुर, राजस्थान

सूचित सहमति पत्र

थीसिस / निबंध का शीर्षक: फुफ्फुसीय अन्तः शल्यता में दोहरी ऊर्जा की गणना टोमोग्राफी।

पी. जी. छात्र का नाम: डॉ सतीश कुमार

दूरभाष।संख्या : 8057617636

रोगी / स्वयं सेवक पहचान संख्या: _____

में, _____

पुत्र/पुत्री _____

निवास _____

निम्नलिखित अध्ययन मे भाग लेने के लिए मेरी पूर्ण, स्वतंत्र, स्वैच्छिक सहमति देता हूँ,
फुफ्फुसीय अन्तः शल्यता में दोहरी ऊर्जा की गणना टोमोग्राफी।

जिसकी प्रक्रिया और प्रकृति मुझे अपनी पूरी संतुष्टिशह अपनी भाषा में समझाई गई है। मैं
पुष्टि करता हूँ कि मुझे प्रश्न पूछने का अवसर मिला है।

मैं समझता हूँ कि मेरी भागीदारी स्वैच्छिक है। मुझे बिना कोई कारण प्रकाशित किये किसी
भी समय अध्ययन से बाहर निकलने के मेरे अधिकार की जानकारी है।

मैं समझता हूँ कि मेरे और मेरे मेडिकल रिकॉर्ड के बारे में एकत्रित की गई जानकारी
को _____ (कंपनीनाम) या विनियामक प्राधिकरणों से जिम्मेदार व्यक्ति देख
सकता है। मैं इन व्यक्तियों को अपने अभिलेखोंकि जांच के लिए अनुमति देता हूँ।

तारीख : _____

जगह: _____ हस्ताक्षर / बाएंअंगूठे का

छाप _____

यह प्रमाणित किया जाता है कि मेरी उपस्थिति में उपरोक्त सहमति प्राप्त की गई है।

तारीख : _____

जगह: _____ पी. जी. छात्र के हस्ताक्षर _____

गवाह 1: _____

गवाह 2: _____

हस्ताक्षर: _____

हस्ताक्षर: _____

तारीख : _____

तारीख : _____

Ethical clearance certificate

No. AIIMS/IEC/2021/3533

Date: 12/03/2021

ETHICAL CLEARANCE CERTIFICATE

Certificate Reference Number: AIIMS/IEC/2021/3368

Project title: "Role of dual energy CT in the detection of pulmonary embolism"

Nature of Project: **Research Project Submitted for Expedited Review**
Submitted as: **M.D. Dissertation**
Student Name: **Dr. Satish Kumar**
Guide: **Dr. Pawan Kumar Garg**
Co-Guide: **Dr. Pushpinder S Khera, Dr. Rengarajan Rajagopal, Dr. Nishant Kumar Chauhan, Dr. Surender Deora, Dr. Gopal K Bohra & Dr. Sadik Mohammed**

Institutional Ethics Committee after thorough consideration accorded its approval on above project.

The investigator may therefore commence the research from the date of this certificate, using the reference number indicated above.

Please note that the AIIMS IEC must be informed immediately of:

- Any material change in the conditions or undertakings mentioned in the document.
- Any material breaches of ethical undertakings or events that impact upon the ethical conduct of the research.

The Principal Investigator must report to the AIIMS IEC in the prescribed format, where applicable, bi-annually, and at the end of the project, in respect of ethical compliance.

AIIMS IEC retains the right to withdraw or amend this if:

- Any unethical principle or practices are revealed or suspected
- Relevant information has been withheld or misrepresented

AIIMS IEC shall have an access to any information or data at any time during the course or after completion of the project.

Please Note that this approval will be rectified whenever it is possible to hold a meeting in person of the Institutional Ethics Committee. It is possible that the PI may be asked to give more clarifications or the Institutional Ethics Committee may withhold the project. The Institutional Ethics Committee is adopting this procedure due to COVID-19 (Corona Virus) situation.

If the Institutional Ethics Committee does not get back to you, this means your project has been cleared by the IEC.

On behalf of Ethics Committee, I wish you success in your research.


Dr. Praveen Sharma
Member Secretary

Member secretary
Institutional Ethics Committee
AIIMS, Jodhpur

